

Vertical Profiling of Currents Using Acoustic Doppler Current Profilers

Chapter Outline

11.1. Basic Assumptions and Operational Issues	340	11.5. Horizontal-Facing ADPs	354
11.2. Principle of Operation	341	11.6. Subsurface Moored ADPs	358
11.3. Profiling Geometries	344	11.7. Downward-Facing Shipboard ADPs	360
11.3.1. Bottom-Mounted, Upward-Facing ADPs	344	11.8. Towed ADPs	363
11.3.1.1. Combination of Surface Currents and Gravity Wave Orbital Velocities	345	11.9. Lowered ADCP (L-ADCP)	367
11.3.1.2. A Single Upward-Facing ADP for Measuring Currents and Surface Waves	346	11.10. ADPs for Current Profiling and AUV Navigation	368
11.3.1.3. Current Profile and Wave Measurements for Operational Applications	350	11.10.1. AUV-Mounted ADPs for Current Profiling	368
11.4. Trawl-Resistant ADP Bottom Mounts	353	11.10.2. ADPs for AUV Navigation	369
		11.11. Calibration of ADPs	371
		11.12. Intercomparison and Evaluation	372
		11.13. Merits and Limitations of ADPs	374
		References	375
		Bibliography	378

In the past, measurements of vertical profiles of horizontal current flows in the ocean were carried out by the use of moored current meter (CM) chains. Maintaining such moorings at large depths in the ocean was found to be difficult and rather expensive. Vertical profile measurements of oceanic currents were indeed a daunting task for several years. Ideally, one might want a single probe that can scan a large water column and remotely measure the vertical distribution of horizontal motions with high vertical resolution. Although freely sinking/rising probes were successfully used for specific studies, time-series measurements with the aid of such probes proved a difficult task. Various difficulties associated with freely sinking/rising probes and the increasing requirement for time-series measurements of vertical profiles of currents led to the development of acoustic Doppler techniques, borrowed from the radar techniques used in meteorology for wind-velocity profile measurements. Although Doppler sonar techniques were investigated several decades ago and were implemented for measurement of ship's speed based on "bottom track" in shallow waters and "water track" in

deep waters (Joseph, 2000), power requirements proved a serious impediment to incorporation of the Doppler sonar techniques in battery-powered self-recording CMs. Availability of low-power microprocessors removed this hurdle, and Doppler signal processing in self-recording moored instruments thus became feasible. This paved the way to the success of stand-alone self-recording of acoustic Doppler current profiler (ADP) development, giving great relief to a wide spectrum of oceanographic communities who are interested in the measurement of high-resolution vertical profiles of ocean currents.

An ADP is a type of hydroacoustic device that measures and records water-current velocities over a range of distances both horizontally and vertically over a range of depths. ADPs are now receiving considerable stimulus from requirements for research in upper ocean processes in the context of climate research, whereas in the shallow-shelf seas, current profiles are needed in connection with the proving of three-dimensional circulation models, navigation, sediment transport, and fluid loading of structures. Gordon (1990) provides a useful bibliography relating to a variety of ADPs up to 1990.

Apart from HF Doppler radar systems (see chapter 4), ADPs are probably the single most significant innovation in oceanography since the mid-1970s. The first commercial ADP, produced in the late 1970s, was an adaptation of a commercial speed log (Rowe and Young, 1979). The speed log was redesigned to measure water velocity more accurately and to allow measurement in range cells over a depth profile. Refined and improved during the 1980s and 1990s, these instruments can now remotely measure both horizontal and vertical profiles of water currents in sequential layers of water columns. The ADPs break up the water-velocity profile into uniform segments or depth cells, often called *bins*. The fact that ADPs can measure flow velocities from such discrete distances (i.e., bins) from the sensor face has led to an almost universal adoption of the instrument within the oceanographic community. Bin lengths and locations are determined by various parameters that set the transmit pulse length, receive window length, and blank after-transmit length. At present, ADPs are used in several offshore renewable energy applications, coastal applications, and offshore oceanographic applications and can be configured for side-looking into rivers and canals for long-term continuous discharge measurements, mounted on boats for instantaneous surveys, and moored on the subsurface and seabed locations for long-term current and wave studies.

11.1. BASIC ASSUMPTIONS AND OPERATIONAL ISSUES

The basic philosophy embodied in the working of ADPs is based on the mechanism of acoustic volume scattering from a cloud of moving scatterers in the flow field and the well-known phenomenon of the Doppler effect. The term *scatterer* encompasses any kind of inhomogeneity in water, including suspended particulate matter, biological organisms (zooplankton), and minute air bubbles (near the sea surface). Any or all of these scatterers are present almost everywhere in the sea. They remain suspended in the water and, on an average, they move at the same velocity as the water particles. Because the suspended particles move along with the water motion, they are assumed to serve as passive tracers of the flow field. Motions of schools of fishes are an exception to this basic assumption, and therefore the presence of fish schools in the acoustic beam gives errors in the water-velocity measurements. However, such errors can be detected from the backscattering strength measurements made by the ADPs, and the erroneous water velocity data can, therefore, be corrected or the erroneous data removed from the dataset.

The physical properties of the transmission medium have a profound effect on system design. Besides simple

spherical spreading, a number of frequency-dependent loss mechanisms are involved in acoustic signal propagation—the effect being to produce a rapid increase of attenuation with frequency (Urick, 1982). Thus, although it is desirable to operate at high frequency to improve Doppler frequency resolution, the working frequency is generally set by the maximum range required.

Transducer quality is essential for data quality. The transducers must be directional (including both narrow-beam and suppressed side lobes) and efficient. The ADPs use large transducers (relative to the wavelength of sound in water) to obtain narrow acoustic beams (typically 3° for 400 kHz transducer or 1.7° for 2 MHz transducer). The acoustic beams focus most of the energy in the center of the beam, but a small amount leaks out in other directions. Because sound reflects much better from the sea surface than it does from the subsurface water layers, the small signals that travel straight to the sea surface through the side lobes of the ADP can produce sufficient echo to contaminate the desired signal from the subsurface water layers.

Echo intensity (EI) is a measure of the signal strength of the echo returning from the scatterers. EI depends on transmitted power, backscatter coefficient, sound absorption in the ambient water body, and beam spreading as given by (Urick, 1996):

$$EI = SL + SV - 20 \log (R) - 2\alpha R + K \quad (11.1)$$

where SL is the transmitted source level (dB/1 μPa at 1 m); SV is the mean volume backscatter strength (dB/m⁻¹); R is the range along the beam (m); α is the absorption coefficient (dBm⁻¹). The term K is an instrument- and frequency-specific constant, and $20 \log (R)$ accounts for beam spreading (outgoing and incoming spherical spreading and increased scattering volume). EI is now routinely measured by ADPs as a bonus parameter to survey the concentration of zooplankton or suspended sediment—useful for biologists and sedimentologists.

Our understanding of the way in which the properties and behavior of individual scatterers determine backscattering properties is as yet incomplete in several respects. Acoustic scatterers at depths in the ocean well below the surface are primarily of biological origin, and scattering strength is therefore dependent on biological productivity. This can vary spatially and temporally, being enhanced in regions of upwelling and in the well-defined scattering layers. Entrained air bubbles (known as *microbubbles*) can provide a substantial scattering mechanism within 10–20 m of the sea surface (Thorpe, 1986), whereas in areas of strong tidal mixing in continental shelf waters, suspended sediments may provide the greatest source of backscatter (Collar, 1993).

Small-scale motions of scatterers relative to each other are of fundamental importance, for these produce changes

in the relative phases of individual echoes, with the consequence that the phase signature from the ensemble will evolve with time, eventually becoming decorrelated from the initial situation. The characteristic time τ_c during which this process occurs is defined as the *scattering correlation time* and it is a function of the acoustic wavelength, scattering volume, and velocities of the insonified scatterers. In most practical measurement situations, the two-way pulse travel time greatly exceeds τ_c as a result of the relatively slow acoustic propagation velocity, and this initially caused noncoherent processing to be adopted, i.e., the signal frequency is estimated each time from the echo generated from individual transmitted pulses (Collar, 1993). Coherent processing is, however, possible in principle and techniques based on multiple pulses, or coded transmissions have since been developed.

As noted in the preceding introductory remarks, ADPs use acoustic energy directed along narrow beams. The backscattered acoustic energy from suspended material in the water column is analyzed to determine the Doppler shift due to the relative motion between the ADP and the suspended material. The beam width and side-lobe energy levels are important aspects of the performance of the ADP. Beam width is characterized at the -3-db level and is measured in degrees of arc. For example, a typical RD 1,200-kHz transducer has a beam width of 1.4° . The main beam lobe contains most of the energy emitted. However, other transducer characteristics such as size and vibration modes generate beam side lobes. These side lobes are typically -40 dB from the main lobe. The characteristics of these side lobes are significant in determining near-surface and near-bottom measurement accuracy.

The ADP beam angles are typically 30° relative to the principal axis of the transducer, and, therefore, the side-lobe energy at 30° from the main beam points toward the surface or bottom when it is deployed in an upward-looking or downward-looking configuration, respectively. The echo return from the sea surface or the seafloor is considerably larger than that from the suspended material in the water. Therefore, even at relatively low side-lobe energy levels, the return signal is strong enough to contaminate the ADP measurements. This energy is received at the same time as the energy from ~ 85 percent of the profiling range (Appell et al., 1991). Accordingly, RD Instruments recommends in their manual not to use measurements acquired beyond 85 percent of the ADP's maximum specified range when surface or bottom reflections are present.

Contamination from side lobes has the effect of biasing the velocity measurements towards zero. The worst-case condition is a mirror surface that would reflect all the energy back toward the receiver. In this case, the surface is not moving and therefore does not Doppler-shift the signal. In actual *in situ* conditions, the results are dependent on sea surface conditions. The angle of reflection with the surface

wave is constantly changing. This means that the amount of backscattered energy received is varying and the moving surface creates a Doppler shift in the signal. The footprint of the beam at the surface and wavelength of the signal may also have an effect. In a downward-looking mode of the ADP, contamination from bottom echoes is a function of bottom characteristics.

11.2. PRINCIPLE OF OPERATION

ADPs operate on the same principle as the meteorological Doppler radar, but the transducers, transmission signals, and the transmission media in these two devices are much different. Accordingly, the complexities in these two systems are also of different nature. The principle on which Doppler profilers operate is as follows: A sonar (which is an active acoustic transducer) transmits a narrow-beam acoustic pulse (of frequency f_t and temporal pulse length τ) through the water in a given azimuthal direction at a known angle to the horizontal: downward from a ship-based installation, upward or downward from a moored instrument, upward from a seabed instrument package, or horizontally from a vertical structure. The transmitted sound pulses from the ADP scatter in all directions from the sound scatterers; most of the sound propagates in the forward direction, unaffected by the scatterers and the small amount that reflects back (i.e., echoes) is Doppler-shifted. After transmission, the same transducer operates as a receiver to receive the echoes from the scatterers, which remain suspended in the water body. The back-scattered acoustic signals are received as a function of time after transmission.

The ADP's automatic gain control (AGC) circuit begins to increase the gain (i.e., amplification) of the incoming signal after transmission of a pulse is completed. This time-varying gain (TVG) compensates for the decreasing strength of the return signal with increasing radial (i.e., along-beam) distance from the ADP. Thus, a single transceiver (i.e., transmitter-cum-receiver) detects the components of water-flow velocity resolved along the acoustic beam of the transceiver. The flow-velocity component along the acoustic beam is known as *radial velocity*.

During the reception sequence, the backscattered acoustic beam, which is oriented in a given direction, is divided into different slant range-gated cells, known as *bins* (see Figure 11.1). By time-gating the stream of received backscattered signals, different radial velocity components v_i

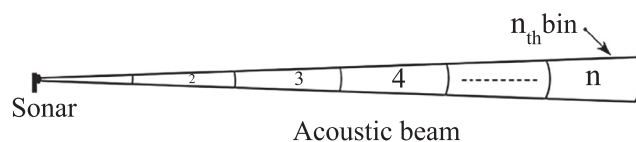


FIGURE 11.1 Range-gated cells, known as bins, of a backscattered acoustic beam, from which radial current measurements are made.

are estimated corresponding to each i_{th} bin. The water motion in a given bin (which is assumed to be the same as the motion of the scatterers in that bin) introduces a Doppler shift $f_D = (f_r - f_t)$ corresponding to that bin, where the transmitted sonar frequency is f_t and the received sonar frequency is f_r . Because the same transducer is used for transmission as well as reception (known as *monostatic configuration*), the Doppler shift f_D can be reduced to a form (see Section 9.3 for details):

$$f_D = \frac{2f_t}{c} v \quad (11.2)$$

where c is the velocity of sound in water at rest ($\sim 1,500$ m/s). From Equation 11.2, the radial flow velocity v in a given bin is estimated as:

$$v = \frac{c f_D}{2 f_t} \quad (11.3)$$

The Doppler shift from a given bin (say, i_{th} bin) is proportional to the radial velocity v_i whose sign is positive or negative depending on whether v_i is toward or away from the transducer. Thus, the Doppler shift of the volumetric echo from the scatterers in the successive bins in the flow field is used to determine the relative radial velocity of the water-current flow in the successive bins along the acoustic beam. Thus, by examining the backscattered signal within discrete preselectable time intervals (range-gated bins) and measuring the Doppler shift within each bin, a time series of the radial components of the water velocity within the maximum attainable range of the ADP can be deduced.

ADP records current-flow velocity as an average of many velocity estimates (called *pings*). The uncertainty of each ping is dominated by the short-term error. Averaging multiple pings as in Equation 11.4 reduces errors (*Aquadopp Current Profiler User Guide*, Nortek AS, Rud, 2005):

$$\sigma_{V\text{mean}} = \frac{\sigma_{V\text{ping}}}{\sqrt{N}} \quad (11.4)$$

where σ is the standard deviation, and N is the number of pings averaged together.

Each acoustic beam measures the flow-velocity component along the beam and does not sense the velocity perpendicular to the beam. ADP measures the full three-dimensional velocity with a minimum of three beams, all pointed in different angular directions relative to the principal axis of the ADP. Under an implicit assumption that currents are horizontally homogeneous (i.e., uniform currents across layers of constant depth), the current velocity vector can be obtained using appropriate trigonometric relations, taking into account the specific beam geometry of the ADP.

The backscattered signal, normally of microvolts in amplitude, is composed of the random sum of the individual scattering amplitudes, each having a Doppler frequency shift associated with the radial velocity (i.e., velocity along

the acoustic beam) of the scatterer. Because the microinhomogeneities that cause the scattering are of random sizes, the received signal is subjected to amplitude modulation. Phase incoherencies also arise as a result of different ranges of the individual scatterers from the acoustic receiver as well as their random motion due to turbulence within the defined scattering volume. The signal is also corrupted by an additive white Gaussian noise. Thus, the received signal is a highly distorted version of the transmitted signal wherein its deterministic properties are no longer valid, and therefore application of nonstatistical methods for extraction of Doppler-shift information has invariably failed. For example, Crocker (1983) investigated an axis-crossing counting technique in which the returned signals were first heterodyned with closely spaced, digitally synthesized local oscillators to produce a narrow base-band frequency, but the method was found to be unsatisfactory. Because the backscattered signal is statistical in nature with Gaussian distributions, a realistic approach for estimation of Doppler-shift information is some form of statistical method. Most of the Doppler-shift information is contained in the first and second spectral moments of the Doppler spectrum.

Extraction of the mean Doppler frequency from the backscattered signal can in principle be achieved in several ways. However, the need for real-time processing in low-powered, self-contained instruments has tended in practice to encourage the application of either fast Fourier transform (FFT) or complex autocorrelation methods on the received echoes. The FFT algorithm provides a description of the spectrum of the received signal (the mean Doppler frequency shift is assumed to be the first moment of the discrete power spectrum, and the second moment is assumed to be a measure of turbulence in the flow field) but requires rather more computation than does the complex autocorrelation method, which is implemented relatively easily. The complex autocorrelation method appears to perform better, particularly at low S/N ratios (Sirmans and Bumgarner, 1975). Thus, realization of an optimum ADP is very dependent on the nature of the problem under investigation. Discussion of the fundamental constraints can be found in Pinkel (1980).

There are many ways to process the velocity data, each with its own advantages and drawbacks. Until now there existed three broad classes of ADP in terms of pulse transmission and processing of the received backscattered acoustic signals: (1) incoherent, (2) coherent, and (3) broadband systems.

In the incoherent system, each of the acoustic transducers of the ADP transmits an ultrasonic acoustic pulse of temporal length τ and receives the backscattered return echoes as the pulses propagate through the water column along the respective slant ranges defined by the acoustic beam. The return signals are slightly shifted in frequency relative to that of the transmitted signal (i.e., Doppler-shifted) by an amount

proportional to the relative radial velocity of the water current. The Doppler-shifted echoes, received at the ADP as a function of time after transmission, yield the relative radial velocity in sequential layers at each of the “range-sliced,” insonified (i.e., acoustically illuminated) volumes of the overlaying water column. By adjusting the transmitted pulse length τ , the portion of the water column insonified at any given instant can be controlled in order to choose the desired range resolution.

For a single-pulse system, as just mentioned, slant-range resolution and radial velocity resolution are closely related. The Fourier transform of a transmitted rectangular pulse of temporal length τ has width $(1/\tau)$. Increasing the pulse length improves the resolution of water-current measurements but simultaneously reduces resolution in range. A limit to this process occurs when the pulse length τ equals the scatterer correlation time; thereafter, range resolution decreases with increasing τ , without any corresponding benefit in velocity resolution. However, it may be noted that the resolution product improves with increasing transmission frequency f_t because, for a given radial velocity v of the flow field, the Doppler shift is proportional to f_t .

A more optimistic lower bound on the attainable measurement accuracy has been derived by Theriault (1986a) based on the Cramer-Rao criterion. Analyses of the performance bounds for practical systems have been made by Hansen (1985), applying several types of velocity estimation algorithms to a series of measured and simulated datasets. The use of coded pulses as a means of reducing velocity variance has been proposed by Pinkel and Smith (1992) and independently by Trevorrow and Farmer (1992). The incoherent method (Doppler processing in terms of changes in frequency) is relatively simpler to implement but suffers from limited space-time resolution.

Unlike the just-mentioned noncoherent processing, coherent processing works in the time domain (not frequency). This method is rather new in ADPs, although it was well established in atmospheric sounding radars (Mahapatra and Zrnic, 1983). Coherent processing ADPs use the phase differences (propagation delays), which are exactly proportional to the particle displacement, and with known speed of sound in the sea and time lag between sound pulses, particle velocity can be computed. In coherent processing, a multiplicity of pulses is transmitted while maintaining phase coherence in the transmitted signal. Doppler shift is evaluated from the pulse-to-pulse change in phase of the received signal, with a frequency resolution that depends on the total dwell time.

Because Doppler resolution is no longer dependent on individual pulse length, in contrast to noncoherent processing, pulse lengths can be chosen to provide a desired range resolution, system, or transducer bandwidth, with S/N considerations alone providing a practical lower limit.

Consequently, coherent systems provide greatly enhanced velocity and range resolution. The ADPs developed from the 1980s onward, incorporating coherent processing method (e.g., Rowe et al., 1986; Lohrmann et al., 1990), are capable of providing precision in oceanic current measurements of a fraction of a cm/s, thereby offering an improvement of two orders of magnitude over noncoherent systems.

Multipulse coherent systems are, however, restricted by ambiguities in both velocity and range. The velocity ambiguity arises because the returned signals are effectively sampled at the pulse repetition frequency, f_{pr} , and the usual sampling theorem considerations apply, i.e., aliasing takes place if the maximum Doppler frequency f_{\max} exceeds the Nyquist limit ($f_{pr}/2$). The maximum velocity that can unambiguously be observed is given by the condition:

$$|V_{\max}| < \frac{|f_{pr}\lambda|}{4} \quad (11.5)$$

Range ambiguity results from the inability to distinguish between the return from a given pulse and the returns from earlier pulses scattered from greater ranges. Maximum unambiguous range is given by:

$$R_{\max} = \frac{c}{2f_{pr}} \quad (11.6)$$

The combination of unambiguous range and velocity thus has the upper limit given by:

$$V_{\max} \cdot R_{\max} = \frac{c\lambda}{8}, \quad (11.7)$$

which is independent of pulse repetition frequency.

The enhanced temporal and spatial resolution available from coherent techniques offers possibilities for determining the parameters of small-scale turbulence, and it is in this context in particular that much pioneering work was done (Lhermitte, 1985; Lhermitte and Serafin, 1984). The major effect of turbulence is to increase the spectral variance of the Doppler signal. Consequently, measurements of the spectral width (given by second spectral moment) as well as the mean (given by first spectral moment) become necessary. Interpretation, however, may be complicated by other contributions to spectral broadening from current shear and by any limitation in target residence time in the acoustic beam (Collar, 1993). The coherent method provides improved space-time resolution compared to narrowband processing by a factor of 2–5, but this method is complex to implement. Coherent processing techniques are discussed by Pinkel (1980) and Rowe et al. (1986).

The use of coded transmissions and application of broadband signal-processing techniques provide a compromise between coherent and the simple incoherent systems. Two such systems have been implemented. Brumley et al. (1991) use correlated pulse pairs; the method adopted by Pinkel and Smith (1992) involves the transmission, within

a pulse, of a number of repeats of a broadband subcode. Doppler shift is estimated from the complex autocovariance of the return at a lag equivalent to the subcode length. The transmission of multitone and of frequency-shift-keying (FSK) waveforms has been investigated by Andreucci et al. (1992). The broadband method allows the number, composition, and spacing of pulses to be varied to achieve different values of velocity measurement precision, but each variation imposes restrictions on profiling range, instrument velocities and dynamics, vertical resolution, and power consumption that must be considered. Improvements in the standard operating firmware and data-recording capabilities and a decrease in overall instrument size and weight also favor the broadband ADP over the narrowband if equivalent performance can be achieved.

11.3. PROFILING GEOMETRIES

Both vertical and horizontal profiles of water-current measurements can be obtained using ADPs of various geometries. These typically include two-, three-, four-, and five-beam systems, wherein the individual transducer heads (and therefore the acoustic beams emitted from them) are divergent (typically 20° to 30°) relative to the principal axis of the ADP (see Figure 11.2). The ADP measures the current relative to itself; therefore, it is necessary to correct the data for ADP attitude and motion. In the case of stationary transducers, the Doppler shifts directly yield the profiles of absolute radial velocity components. If the

transducers are nonstationary (e.g., mounted on a buoy or at the bottom of a ship), the absolute water-velocity profile can be obtained from knowledge of the motion of the transducers. Incorporation of a magnetic compass enables the ADP to convert velocity measurements to Earth coordinates (i.e., *east, north, and up*, or ENU, components). To obtain the ENU components, the ADP first converts the data to XYZ coordinates (i.e., orthogonal coordinate system relative to the ADP) and then converts them to the Earth coordinates using tilt and heading data.

The accuracy of water-current speed measurement depends on the incorporation of correct measurement of the speed of sound in still water, the transmission angle, and the accuracy with which the Doppler shift is estimated. The speed of sound c (m/s) in seawater is a function of water temperature t (°C), depth d (m), and salinity s (parts per thousand), as approximately given by:

$$c = 1449.3 + 4.572t - 0.0445t^2 + 0.016d \\ + 1.398(s - 35) \quad (11.8)$$

Thus, an incomplete understanding of the *in situ* sound speed in seawater at rest directly affects the water-current velocity estimation, often dominating the error sources. The ADP usually obtains the speed of sound in seawater by assuming a nominal salinity and computing the sound speed based on the measured temperature and transducer depth. The process works relatively well because sound speed in seawater at rest is more sensitive to water temperature than it is to salinity. A pressure sensor is also needed for the measurement of deployment depth for a moored ADP. Because the velocity of sound in seawater at rest is about 1,500 m/s, a water-current velocity profile over the entire range of the profiler is obtainable within a few minutes, even after averaging over many samples.

11.3.1. Bottom-Mounted, Upward-Facing ADPs

Remote monitoring of seawater currents and sea surface waves in the near-shore region is of great interest, both academically and to the general public, because of the role of these currents and waves in coastline erosion and their impact on recreational activities. Making measurements in coastal regions rich in tidal energy is a challenging and potentially dangerous task. Not only do tides run at such high rates that environmental windows—i.e., the only times when it is possible to deploy and recover measurement instrumentation—are extremely narrow, but regions of large tidal currents commonly have whirlpools and standing waves due to huge velocity shearing, which makes safe navigation particularly difficult. In a vertically sheared current profile in coastal waters, the current may be very strong at the surface and much slower at the bottom.

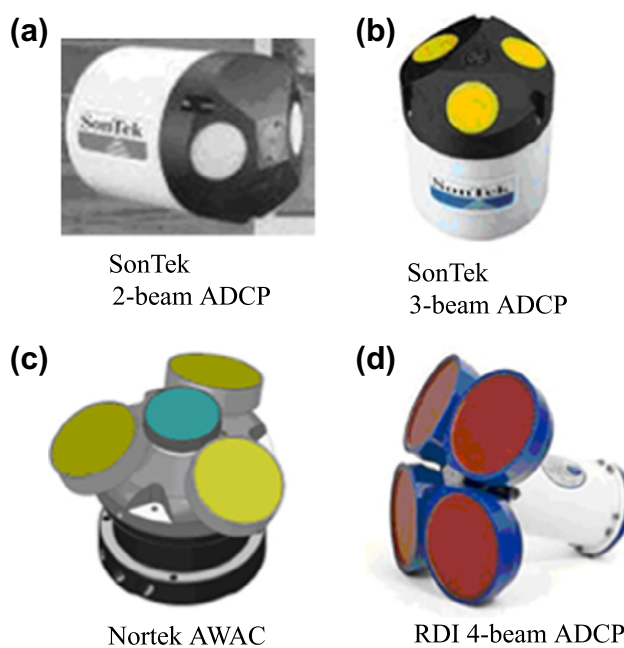


FIGURE 11.2 ADCPs of various geometries, wherein at least two of the acoustic beams emitted by the individual transducers are divergent (typically 20° to 25°) relative to the principal axis of the ADP.

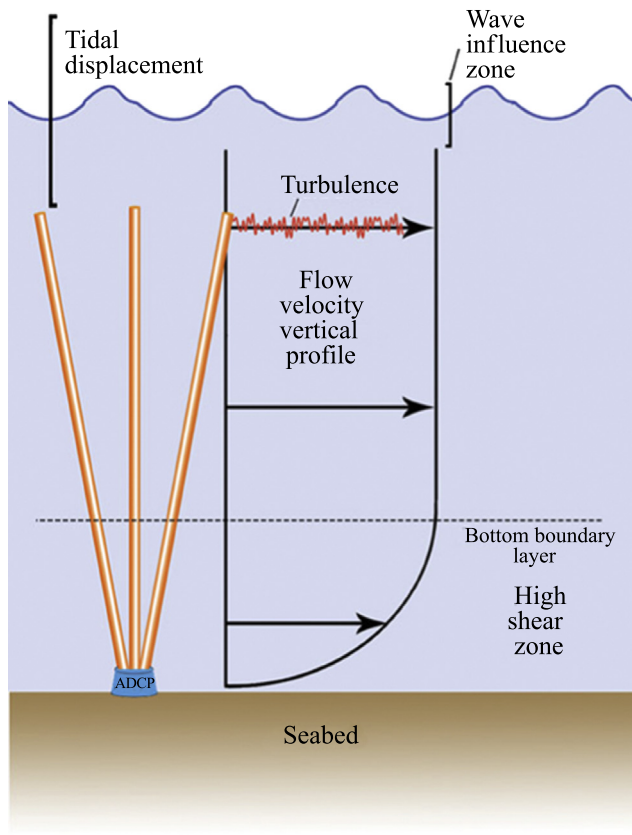


FIGURE 11.3 Schematic diagram showing the vertical current velocity profile in shallow coastal waters. (Source: Wilson, 2009, International Ocean Systems, www.intooceansys.co.uk.)

Furthermore, highly chaotic current/wave conditions can prevail where there is wind against tidal propagation, where there are dramatic variations in bathymetry, or during storm-surge events. As the current profile in shallow coastal

regions (see Figure 11.3) is influenced by several factors, such as bottom boundary layer, tidal displacement, wave influence, and the like, high-frequency ADPs capable of high-resolution profile measurements (see Figure 11.4) need to be deployed for capturing all these variabilities occurring in a relatively small water column. Placing equipment on the seabed in the hostile conditions of the coastal waters is challenging. Therefore, a single instrument package that can measure multiple parameters is of great practical utility to both technologists and user communities.

11.3.1.1. Combination of Surface Currents and Gravity Wave Orbital Velocities

Water currents at the topmost layers of the ocean are a combination of surface currents and orbital velocities of surface gravity waves (wind-driven waves). In shallow water, the relationship between the vertical and horizontal components of water-flow velocity changes with depth, because wave orbits are approximately circular near the surface (i.e., the magnitudes of the vertical and horizontal components of velocity are approximately equal), but near the bed the orbits are horizontal (the vertical velocity is zero or near zero). In the past, bin-averaged, Earth-referenced vector-current measurements provided by shallow-water ADPs led to some confusion among some inexperienced users who were previously familiar with water-current measurements provided by conventional Eulerian-style CMs only, which do not have the ability to measure sea surface wave orbital velocities, although the water-current measurements provided by such CMs are often contaminated in varying degrees by wave motions. Fortunately, probably in an attempt to provide more clarity on shallow-water ADP measurements, Howarth (1999) reported the raw measurements (individual

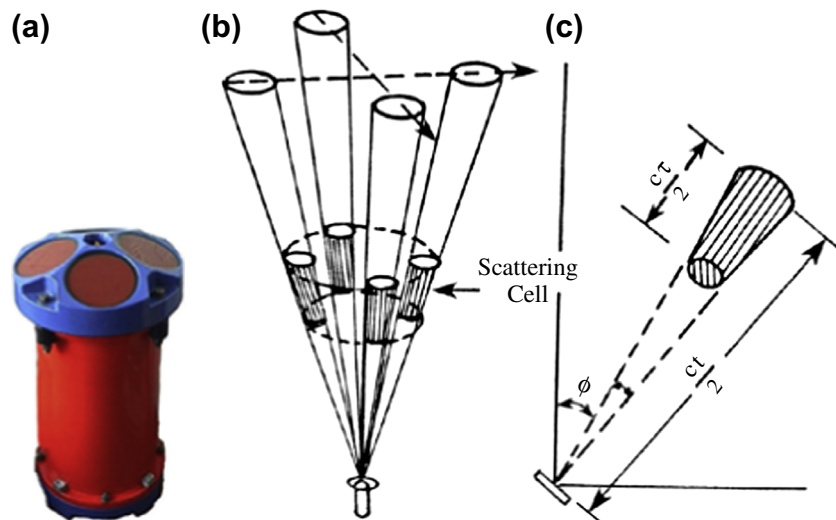


FIGURE 11.4 (a) A four-beam ADCP in Janus configuration; (b) upward-looking slanted beams from the ADCP and the scattering cells in a horizontal plane; and (c) expanded view of a typical scattering cell. High spatial resolution is achieved by the use of small value for τ .

measurements from each bin of each beam) obtained from a standard four-beam, 1.2-MHz ADP deployed in a seabed frame in Red Wharf Bay, off Anglesey in the Irish Sea, in a water depth of 23 m at low water. In this dynamic (tidally stirred) environment, there were sufficient scatterers (sediment) for there to be a good signal in all 20 bins. However, data quality in the uppermost two bins (bins 19 and 20) was affected by side-lobe interference from the sea surface return around low water. The instrument sampled every 2 seconds for 25 hours, recording beam data in 20 1-meter bins from 3.6 to 22.6 m above the bed (the beams were at 20° to the vertical).

To gain a quick impression of the data content and quality, preliminary data analysis was carried out by splitting the records from each beam and for each bin into 10-min blocks (300 samples) and calculating means and standard deviations. Ten-minute blocks have been shown to be a sensible partitioning of the record so that each block includes sufficient high-frequency events (waves and turbulence) for analysis, at the same time as being stationary with regard to the tides (Soulsby, 1980). The “means” clearly shows the tidal signal. It is interesting to note that the standard deviations also exhibit an identifiable signature in which amplitude increases with height above the bed. This contrasts with the deployments in deeper water, where tidal currents were weak, which showed no differences between the bins, or with time, and standard deviations were mainly in the range 10–15 mm/s, as would be expected given the ensemble standard deviation. The patterns illustrated in respect of beam 3 were exhibited by all four beams, both in the vertical and with time. The signal was highly coherent with depth and oscillatory with a period of about 5.5 s.

During a stormy period, the standard deviations decreased exponentially with depth, in which all bins are plotted. The deployment and measurement schemes adopted by Howarth (1999) revealed the finer intricacies of measurements actually performed by the ADP in shallow waters. For example, wave activity, with peak periods of between 5 and 6 seconds, was detected in the top bins throughout the record. The largest wave activity occurred during low water, when wave orbital velocities were twice as large as for the rest of the deployment. During low water, wave activity was detected in all current bins, decreasing exponentially with depth.

To some pessimistic users who lacked acumen and have no nose for knowing the unknown, the ADP measurements as described would have been “instrument noise” or a result of “deployment error.” However, to some erudite technologists and devoted researchers with a nose for mining the hidden treasures from the deep, the “noise” was indeed an invaluable signal. These technologists and researchers realized that, clearly, sea surface wave orbital velocities were being measured, and the shallow-water ADP measurements are indeed a combination of currents, wave orbital velocities,

and turbulence. This was realized in the late 1980s, and this realization ultimately culminated in the invention of the now-famous seminal piece of oceanographic remote sensing equipment known as a *directional wave-measuring ADP*. These aspects are addressed in Section 11.3.1.2.

This discussion indicates that the presence of waves, turbulence, and currents in the wave zone, as well as the mutual influence between them, need to be understood and properly taken into account when profilers such as shallow-water ADPs with the capability for detection of currents and high-frequency events (wave orbital velocities and turbulence) with high spatial resolution in the vertical are deployed in shallow waters.

Because water motions at the topmost layers of the ocean are a combination of surface currents and orbital velocities of surface gravity waves (wind-generated waves), fast-sampled (of order 1 Hz) high-frequency (1 MHz or higher) ADP measurements in shallow water offer the prospect of estimating high spatial resolution surface currents and several wave parameters that are difficult to measure by other means: wavelength, wave direction, and the decay of wave energy with depth as well as the standard time-series determination of wave period from individual bin measurements (Terray et al., 1990; Gordon et al., 1998).

In a vertically sheared profile, the current may be very strong at the surface and much slower at the bottom. Taking these into account, it is appropriate to obtain the estimates of an integrated mean surface current by creating a weighted average of the ADP current profile relative to the depth penetration of the wave. The depth-average current U can be estimated from the vertically sheared current $U(z)$ using the expression (Kirby and Chen, 1989):

$$U = \frac{\int_0^0 U(z)E(\omega, z)dz}{\int_{-H}^0 E(\omega, z)dz} \quad (11.9)$$

where ω is the bottom-relative radian frequency of the wave, H is the water depth below the surface, and E is the wave energy. The specialty of the ADP is that it is particularly useful in measuring the current profile over the region in which wave energy is concentrated.

11.3.1.2. A Single Upward-Facing ADP for Measuring Currents and Surface Waves

Historically, the technology for measuring ocean currents and sea surface gravity waves has been distinct, requiring separate instrumentation for each. For instance, it is quite common to measure sea surface waves from a surface-floating buoy (wave rider buoy). However, there are some

locations that preclude such measurements on practical grounds, as well as many other locations that present challenges to the survivability of surface buoys. The challenges include shipping traffic, vandalism, and ice cover. One alternative to wave measurements is to measure pressure from below the sea surface. The method has shown good results; however, it is limited to shallow coastal waters (because short gravity waves attenuate with depth) or to measurements of only long waves, such as tides and tsunami waves. Notable developments have improved on the earlier shortcomings.

Fortunately, research initiated in the 1980s and continuing into the 1990s and beyond (e.g., Krogstad et al., 1988; Terray et al., 1990; Herbers et al., 1991; Zedel, 1994; Visbeck and Fischer, 1995; Terray et al., 1997; Terray et al., 1999; Pedersen and Lohrmann, 2004) showed that apart from the well-established capability of the ADPs for remote measurement of horizontal and vertical water-current profiles, they can also be used for measuring sea surface wave height and direction from a single upward-looking multibeam ADP package deployed in shallow depth relative to the surface.

As indicated earlier, ADPs intended for vertical profiling of water currents employ acoustic beams inclined at an angle relative to the vertical (typically by 20–30°). The sonar measures the instantaneous water-velocity component projected along each beam, averaged over a range cell. Because the “mean” current is typically horizontally uniform over the beams (horizontal homogeneity is assumed, at least), its components can be recovered as linear combinations of the measured along-beam velocities.

Application of ADPs for Sea Surface Gravity-Wave Measurements

The ADP measures sea surface waves using three independent techniques for redundancy (Terray et al., 1999). The primary method of wave measurement is profiling the orbital velocity of the wave. The ADP uses the along-beam component of the orbital velocity for each depth cell to construct a virtual array (the collection of ADP range cells constitutes the array). In a four-beam ADP, there are six different combinations of pairs of beams, any two of which allow the calculation of the wave direction and the wavelength for each bin. Array-processing methods are then used to estimate the direction of wave arrival.

Although traditional current profiling expects horizontal homogeneity, wave measurement capitalizes on the phase differences inherent in a spatially separated array of sensors. Cross-spectra are calculated between every sensor, and the directional spectrum is assumed to be linearly related to the cross-spectra. The cross-spectra will give the phase differences between the various beams. From the phase differences, the wave direction and wavelength can be calculated by simple trigonometry based on the beam

geometry of the ADP. The procedure used here for wave-direction estimation is similar to that used in HF Doppler radar technology for current direction estimation (see chapter 4). Linear wave theory is used to translate the measurements from velocity spectrum at various depths to surface displacements (Note that surface displacement is the time-integral of orbital velocity). Orbital velocity provides a measure of both directional and nondirectional waves. Because the ADP wave gauge automatically chooses depth cells below the surface, even when the surface moves with tides, wave measurements based on the orbital velocity estimates are of high quality, even during hurricane events. This was noticed in the ADP-based wave measurements during hurricane Lili.

Although fast-sampled, high-frequency ADP measurements of wave orbital velocities in shallow water offer the prospect of measurements of surface gravity wave parameters in a novel perspective, interpretation of such measurements is difficult, both because the ADP measures the component of speed along the beam toward the ADP (neither the vertical nor the horizontal component, but one at an angle to the vertical) and, of greater consequence, the ADP beams diverge. Whereas the separation of the beams is not significant in measuring currents averaged over periods of a minute or longer, beam separation is important for studies of waves, because the separation at the surface can be a significant fraction of the wavelength, hence making it impossible to resolve the pairs of opposing beam velocities sensibly into the vertical and horizontal components of the wave orbital velocity. This also means that to study waves, velocities should be recorded in beam coordinates and not Earth coordinates. A consequence of the angling of the beams is also that vertical profiles are not directly measured. The separation of the beams is, however, turned to advantage, and the array of multiple beams is used to estimate wave direction and wavelength from the phase differences between the beams. Because the lower bins (i.e., those closer to the ADP) are closer together horizontally, the phase differences between the beams should be smaller there.

The second technique is the surface track. This is simply echo location of the range to the surface and is an excellent nondirectional ground truth because it is a direct measure of the surface and does not depend on wave number.

The last measure of nondirectional spectra is the pressure sensor. This method has a long history but is very sensitive to wave number. Having three independent sources of wave spectra in one instrument allows one to identify error sources and ensure data quality. The three spectra should agree very closely.

The conventional slant-beam configuration can be used to determine the water column vertical height above the ADP and, therefore, the wave height. Based on several field measurements, it was realized that the slanted-beam configuration of the ADP for wave-height measurements

does not work well during periods of swell. It is generally agreed that for wave-height determination by an ADP, one of its acoustic beams needs to be oriented vertically (Zedel, 1994; Visbeck and Fischer, 1995). The reason for this preference is that a vertical beam for acoustic surface tracking (AST) provides reliable direct measurement of the distance to the surface and thus an estimate of the surface position under almost all wind and wave conditions. In particular, for the so-called “Bug-eye” 3+1 beam configuration (see Figure 11.2c), the vertical wave velocity (which is nondirectional) can be used to estimate the wave-height spectrum (Zedel, 1994) with a slight improvement in performance over conventional Janus type slant-beam ADPs (Terray et al., 1999).

AST is central in the ADP-based wave measurement scheme, to which there are several benefits (Lohrmann and Siegel, 2010):

- Wave processing is much simpler because the estimate of distance to the surface (AST) is free of any complex transfer functions and therefore it provides a direct estimate of the sea surface variations.
- Unlike sea surface wave-related parameters such as pressure and velocity, the AST retains high-frequency wave information because it is not lost by attenuation.

A direct estimate also means that a time series of the sea surface elevation is available to calculate estimates of $H_{1/3}$, $H_{1/10}$, H_{\max} , and T_{mean} . Furthermore, it is unaffected by mean currents that impose a Doppler shift on the surface waves (see the principle of HF Doppler radar technique used for surface current measurements)—a result requiring special consideration when calculating the frequency-dependent transfer function for the velocity and pressure. Perhaps the most important benefit is the simple fact that wave resolution (shorter wave information) is only mildly affected by increased deployment depth.

However, it must be noted that although the response is mild, some high-frequency wave information is lost at greater depths. The extent of the high-frequency filter is determined by the size of the sea surface area ensonified (sampled) by the AST pulse. For a given beam width, the diameter or “footprint” of the ensonified area increases as the vertical distance (i.e., depth) from the surface increases. When the diameter of this footprint becomes similar in size to a wavelength of the sea surface wave, then the structure of the waveform (crest and trough) cannot be well resolved. There is an averaging of the distance over the waveform and thus a “smearing” of the true features. A “cut-off” frequency is assumed when the footprint diameter is equivalent to half a wavelength (of the sea surface wave).

Within the limitations just indicated, the AST solved the depth limitation for nondirectional wave measurements, but the limitations for direction waves still remained. Estimation of wave direction is more complicated than

wave-height determination. This complication stems from the fact that, unlike tsunami waves, the surface gravity waves are not spatially coherent and the waves at any given instant arrive from multiple directions.

In the state-of-the-art acoustic Doppler method, the directions of arrival of sea surface waves (i.e., wave directions) are estimated by using several measurements of wave orbital velocity, together with the AST. As mentioned earlier, the collection of ADP range cell measurements form an array projected from the ADP to just below the sea surface. A number of methods have been invented to estimate the direction of multiple arrivals using sparse arrays (e.g., Johnson and Dudgeon, 1993). Terray et al. (1999) used an iterative version of Capon’s Maximum Likelihood Method (Capon, 1969), known as the Iterative Maximum Likelihood Method, or IMLM (Krogstad et al., 1988; Pawka, 1983). This technique has the advantage that it does not require that the array be uniformly spaced. Iteration improves the consistency of the MLM estimate in the sense that the estimated directional spectrum produces cross-spectra in closer agreement with the observations. The result is to sharpen the directional resolution and decrease the side lobes. Like all high-resolution, direction-of-arrival estimators, the MLM is model-based and requires a relation between the frequency-direction spectrum and the array covariance. For example, Strong et al. (2003) estimated the wave directional spectrum by the IMLM, which requires a model of the ADP response, $H(\mathbf{k})$, to a monochromatic wave propagating at an arbitrary angle. Consequently, at each frequency they computed $k(\omega, \alpha)$ over all angles from 0 to 360° (typically at 4° increments) and use this to determine the response function H . In this, k is the bottom-relative wave number; ω is the bottom-relative radian frequency; and α denotes the included angle between the directions of wave propagation and the current.

The array-processing method (the MLM) exploits the time lags between spatially separated measurements of the array in order to estimate direction. Alternatively, the same data may be used in the form of “classic” triplet processing (**SUV**), in which the triplet is formed by the AST (i.e., distance to the surface, S) and two mutually orthogonal horizontal components of orbital velocity measurements (U and V). Both of these directional-processing methods rely on orbital velocity measurements. The frequency-dependent response of orbital velocity with depth determines the frequency resolution for wave directions.

Orbital velocities attenuate exponentially with depth, and this behavior is more severe for higher-frequency waves (short waves). This means that the further down in the water column that the orbital velocities are measured, the less high-frequency information is available. This is the classic problem faced by bottom-mounted instruments, and it may be noted that even the ADP class of instruments suffers from this challenge if it is not managed effectively.

Managing the response means positioning the measurement cells as close to the surface as possible while ensuring that there is no contamination from the surface, either directly from the cells touching the surface or indirectly from side-lobe energy that leaks off the main beam. This can be managed by positioning the cells just below the surface by a fraction of the measured depth; 10 percent of the depth has proven to provide a good signal response without contamination (Lohrmann and Siegel, 2010).

It is important to note that the limitation for the directional estimates is also imposed on the nondirectional estimates if orbital velocities are used to estimate the energy density spectrum. An accurate directional estimate is required if the surface wave is to be estimated accurately for each individual beam. This is why the AST remains the primary estimate and the orbital velocity a secondary estimate for energy.

A second limitation imposed on the resolution for directional estimates is associated with the spatial separation of the measurements. Wave-directional estimates become ambiguous when the horizontal separation is equal to half a wavelength. The result is that waves at the associated frequency cannot be accurately estimated. One perceived solution is to position the measurement cells closer to the ADP such that the horizontal spatial separation between the cells located on a given horizontal plane is reduced; consequently, the surface wave frequency at which this ambiguity occurs is higher. Unfortunately, moving the measurement cell further down in the water column means that the orbital velocity signal disappears due to the well-known sea surface wave attenuation with increasing depth. The result is that there is no performance gain by drawing the cells in closer to the ADP.

In practice, at any instant the wave velocities vary spatially across the array. As a result, except for very long waves that remain coherent during their passage through the array, it is not possible to separate the horizontal and vertical wave-velocity components. However, the wave field is statistically stationary in time and homogeneous in space, and therefore the cross-spectra between velocities measured at various range cells (either beam-to-beam or along each beam) contain information about wave direction. Terray et al. (1999) demonstrated that wave height and direction spectra compare well with a co-located array of pressure gauges.

Although it is true that the collection of ADP range cells constitutes an array, it is a somewhat peculiar one (Terray et al., 1999). First, the S/N ratio in the measured wave velocities varies with depth. At a particular frequency, this variation is due primarily to the vertical decay of the wave energy and (to a lesser extent) on the acoustic S/N ratio, which itself is a function of range. Second, the velocity measured by the ADP is a linear combination of horizontal and vertical wave velocities, with relative weights that depend on both the propagation direction of the waves and the height of the measurement cell above the bottom. For

example, in deep water, as the surface wave direction varies from 0 to 90°, the measured along-beam velocities vary by only 25 percent. Finally, because the range cells closest to the surface have the highest wave velocity S/N ratio, the usable array lag distribution is quite sparse, consisting of long lags from beam to beam and a second group of shorter lags between range cells along each beam. It is quite clear from these considerations that unlike conventional point sensors, the “sensor array” made up of the range cells associated with an upward-looking ADP does not have a simple relationship with the low-order circular moments of the wave directional distribution, and therefore recovering wave direction is considerably more complicated in this case. In any event, the limitations for directional waves require addressing the issue of getting the measurement cells (for orbital velocities) closer to the surface, where the signal is less attenuated by depth.

Strong et al. (2003) observed that the standard ADP wave-processing software (WavesMon) provides accurate spectra and parameters by applying the Doppler-shifted dispersion relationship:

$$(\omega - kU\cos\alpha)^2 = gk \tanh(kH) \quad (11.10)$$

where ω and k are the bottom-relative radian frequency and wave number (i.e., those observed in a fixed reference frame), H is the water depth, U is the current, and α denotes the included angle between the directions of wave propagation and the current U . Note that Equation 11.10 is just the usual dispersion relation for arbitrary water depth applied to the frequency observed in a reference frame moving with the current. In contrast, other methods of wave measurements showed significant wave-height errors greater than 50 percent for hurricane Lili. This indicates that caution should be exercised in interpreting historical wave height data because it is unlikely that storm surge was taken into account.

Based on persistent research, combined wave- and current-profiling ADPs have now been operationalized to a great level of success. The combined acoustic wave and current (AWAC) profiler system developed by Nortek (see Figure 11.2c) is one such instance. This variant of the traditional ADP has managed to circumvent the classic limitations of measuring short surface gravity waves in deep waters by introducing a vertical beam that directly measures the height of the water-air interface (waves) above the instrument. In the combined wave and current profiling ADPs, acoustic Doppler measurements (standard for an ADP) are used for construction of current profiles; a dedicated vertical narrow beam for AST and near-surface Doppler velocity measurements are together used for wave measurements. The AST method traces the surface wave height profile as it passes through its field of view.

The AWAC, which is intended for greater deployment depths and profiling ranges, is a dual-frequency instrument whereby the off-vertical beams used for current profile

measurements transmit at 400 kHz and the vertical beam used for AST transmits at 600 kHz. The vertical beam transmits at a higher frequency in order to maintain the beam's narrow opening angle (1.7°). This same vertical beam has also demonstrated that it is capable of measuring the distance to the water-ice interface, and as a result it can be used as a means to estimate ice draft or ice thickness as well from more extreme latitudes, where the presence of ice is more common (Lohrmann and Siegel, 2010). The wave-burst measurement contains detection methods for both water-air and water-ice interfaces, thereby allowing it to transition seamlessly from wave measurements in the summer to ice measurements in the winter. The AWAC can measure waves and currents over a full depth of 100 meters.

Lohrmann and Siegel (2010) have reported the depth-response evaluation test results of 400-kHz and 600-kHz AWAC wave measurements for both the AST and wave-directional processing, wherein the former and the latter were deployed at 90 and 19 m water depth, respectively, at two spatially separated locations south of Oslo Fjord, which opens to the North Sea. According to them, the AST proved to perform remarkably well. The test period of 10 days provided 240 wave bursts, each of which contained 2,048 samples. Most bursts had no false detects, and the maximum number of false detects was three samples in a single wave burst. The surface wave-frequency resolution associated with the ensonified footprint on the sea surface was consistent with the estimates from the AST beam width and range.

It was observed that there is a low-frequency noise floor for the wave measurements. One explanation for the perceived low-frequency energy is that there are greater fluctuations of the speed of sound (induced primarily by water-temperature fluctuations) as different masses pass over the AWAC during the wave-burst measurement. These fluctuations manifest themselves as variations in the overall range, albeit small relative to the surface wave variations.

Ice Thickness Estimation

Ice thickness estimates from the subsurface require an accurate depth estimate and an accurate distance measurement (AST). To fulfill this requirement, the AWAC now has a temperature-compensated pressure sensor to reduce the uncertainty in the pressure measurements. The AST measurements have been modified by including a second ranging estimate by using a special filter for the water-ice interface, which is different than that used for detecting the water-air interface. Either ice or wave processing can be performed because both estimates are reported within the same wave burst. This makes it ideal for year-long deployments at extreme latitudes where the same measurement scheme is used for waves in the summer, ice thickness in the winter, and both during the transitional periods in the spring and fall.

If an absolute pressure sensor (one that measures subsurface pressure and barometric pressure) is used for subsurface pressure measurements, care has to be exercised while interpreting the ice thickness estimates, because an absolute pressure sensor does not discriminate between subsurface pressure and barometric pressure. Thus, barometric pressure needs to be subtracted from the absolute pressure measurements to obtain the subsurface pressure of interest. Failure to do this will result in contamination of wave and ice thickness measurements.

The 400 kHz AWAC's estimates of significant wave height (H_{m0}) and peak period (T_{peak}) showed good agreement with that of the nearby 600 kHz AWAC. Peak periods are as short as 2 s and the wave heights as little as 30 cm. The directional estimates show a greater variability and not quite as good agreement. There is a notable difference in the first and second half of the deployment. The first half shows a consistent direction from the south-southwest, whereas the second half exhibits a random distribution of the estimates. The reason for this is that the peak period shortens from 8 s to less than 4 s. When it reaches 4 s, the orbital velocities at depth are no longer measurable. Here we witness the frequency limit for directional estimate at approximately 4 s for a deployment depth of 90 meters. The two AWACs have an apparent bias of the wave directions for the first half of the deployment, for which the most plausible explanation is refraction that occurs between the spatially separated AWACs.

11.3.1.3. Current Profile and Wave Measurements for Operational Applications

The unique capability of upward-looking near-surface-deployed ADPs for measurement of vertical profiles of horizontal velocities and surface wave parameters can be effectively utilized for several academic investigations and operational applications. However, for such measurements from shallow coastal regions, ADPs in seabed-mounted frames are required. Use of frame-mounted ADPs requires careful attention because the equipment needs to be located on a stable region of the seabed and in a stable configuration, and it needs to stay in the spot where it is deployed. The ADP needs to remain vertical, which may require frames of specialized design (see Figure 11.5) and possibly divers during deployment to finalize positioning. To ensure recovery, acoustic release units (which can be actuated from a boat or a vessel) should always be integrated into the frame. Bottom-mounted platforms have proven to work well on condensed bottom sediments in relatively shallow water depths.

Requirements are also increasing for real-time current and directional wave measurements at offshore sites in support of oil exploration, wind, wave, and tidal energy production as well as commercial and research ocean



FIGURE 11.5 A Nortek AWAC profiler instrument being deployed on a bottom frame in the Gulf of Mexico. (Source: Siegel, 2007, Ocean News & Technology, www.ocean-news.com.)

observing systems. There are many challenges to operational systems that provide real-time data. Siegel (2007) has reported on new hardware products and measurement techniques that have been developed by Nortek (USA) to provide robust solutions for these demanding offshore requirements.

In shallow, coastal environments (less than 50 m depth), a common solution for current and directional wave measurements is to deploy an ADP on the seafloor. Keeping the equipment away from the ocean surface provides several advantages, such as reduced exposure to harsh storms, security from theft or vandalism, and protection from ships, ice, or drifting debris. Historically, wave-rider surface buoys and fixed-mounted equipment such as wave staffs and wave radar systems have been used for making sea surface wave measurements in offshore regions (deeper than 50 m). At this depth, bottom-mounted ADPs do not provide the directional resolution necessary for research and commercial wave-measurement requirements. Mounting an acoustic system on a subsurface buoy or underwater directly to an offshore platform would permit the instrument to be close enough to the surface for high-quality wave measurements, yet be removed from the dangers of exposure at the surface. There was a dearth of commercial off-the-shelf solutions to meet this requirement.

The AWAC is designed for the special purpose of being mounted directly to a subsurface structure on an offshore platform. The resulting design, commonly known as the Platform Mount AWAC, employs four acoustic transducers asymmetrically arranged on one hemisphere of the system (see Figure 11.2c) to point away from the offshore platform. The three slanted beams are used for current profile and wave

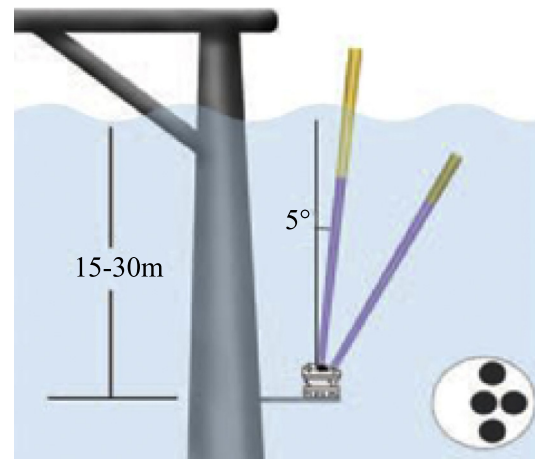


FIGURE 11.6 Platform-mounted AWAC with asymmetric transducer head for deployment on an offshore structure. (Source: Siegel, 2007, Ocean News & Technology, www.ocean-news.com.)

directional estimates, and the fourth (vertical) beam is used to measure wave height. This permits the Platform Mount AWAC to be deployed underwater directly to an offshore structure while at the same time measuring the waves and currents away from the structure (see Figure 11.6).

The upward-looking Platform-Mount AWAC is typically deployed 15–30 m below the sea surface. A downward-looking ADP can be placed below the AWAC to extend the current measurement range into deeper waters (see Figure 11.7). A cable running to the Platform Mount

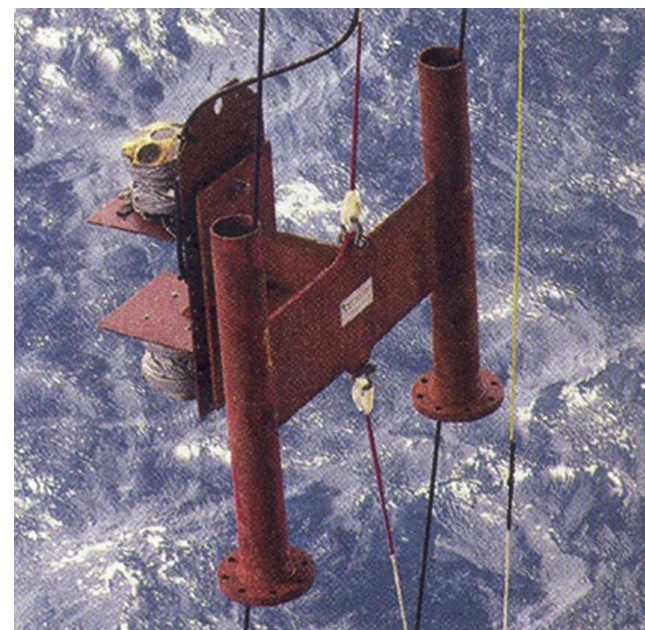


FIGURE 11.7 Platform-mounted AWAC being lowered into place on an oil platform. Downward-looking AWAC is used for current profile measurements into deeper water. (Photo: B. Magnell, Woods Hole Group. Source: Siegel, 2007, Ocean News & Technology, www.ocean-news.com.)

AWAC provides power to the system and transmits data from the AWAC to a computer or telemetry node on the platform. The first such unit was deployed in 2006 on the Ambrose Light Coastal-Marine Automated Network (C-MAN) Station (offshore New York harbor) operated by NOAA's National Data Buoy Center (NDBC); it transmits processed data to the shore by satellite. Real-time wave data from this AWAC are available on the NDBC Website.

Real-time water current and surface gravity-wave measurements from offshore structures may provide critical decision-making data for safe personnel and vessel operations as well as long-term wave-loading information for facility design, maintenance, and repair planning. Future applications could include real-time dynamic feedback loops for optimizing wave energy-harvesting systems, such as real-time modifications of the harvest system based on parameters such as wave height or peak period.

Offshore wave measurements are often needed for site surveys during the planning stages of petroleum and renewable energy projects as well as for fixing boundary conditions for wave models. Sea surface wave buoys have been a common solution to meet these requirements; however, surface buoys may be damaged by storms, ice, and ships. In addition, there are many places in the world that surface buoys would be vandalized or stolen. The ability to mount an ADP for wave measurements on a subsurface buoy would permit the instrument to be close enough to the surface for high-quality wave measurements yet be removed from the dangers of exposure at the surface (see Figure 11.8). However, a subsurface buoy will both

rotate and translate during a wave-sampling period of 10–30 minutes. For this reason, it is not possible to measure waves with a typical ADP deployed on a subsurface buoy without modifying the wave-processing algorithms developed for stationary systems. Nortek managed to resolve this problem by introducing a method called *SUV* (*Siegel, 2007*), addressed in Section 11.3.1.2.

Real-time current and wave data are critical for safe operations at sea and assimilation with nowcast and forecast models. The two most common methods of underwater data telemetry are cables and wireless underwater acoustic modems. Rugged cables may be used to transfer data from a Platform Mount AWAC up to a data collection station on the platform. This cable may also provide power to the AWAC for long-term measurements without the need to change batteries.

Wireless underwater data telemetry solutions are required for instruments mounted in areas where cables are not suitable. This includes regions where bottom trawling is common, on subsurface buoys, and in other situations where cables are impractical because of time or cost constraints. Nortek uses a modified version of the Benthos modem to transmit data from the AWAC to a receiving station such as an offshore platform or surface buoy. The horizontal distance between the acoustic modems can range up to 1–3 km, depending on several environmental factors such as local bathymetry, hydrography, and environmental noise.

Underwater acoustic modems operate at low data transfer rates (typically 300–9,600 baud). To address the increasing need for wave data passing through low-bandwidth channels, Nortek developed the Nortek Internal Processor (NIP). The NIP is a scaled-down PC running a Windows CE operating system. Small enough to fit within the AWAC, it processes the raw AWAC data into a user-selectable set of current-velocity profiles, wave parameters, and energy spectra. These processed data are considerably reduced in size (0.1–1.0 kilobytes) compared with the raw wave data (25–50 kilobytes) and can be easily transmitted through the Nortek underwater acoustic modems. Data formats can be adapted to the user requirements and can be scaled for satellite transmissions.

It has been indicated that the power of the ADP can now be used to obtain wave data while also measuring current profiles. This has been capitalized on by several competing manufacturers. For example, RD Instruments Inc. reported the availability of a new patented capability as an upgrade for RDI WorkHorse ADCPs (*Strong and Devine, 2000*). They reported results demonstrating high-quality output from the ADP wave analysis. In particular, it has been found that ADP wave data do not suffer from biases in significant wave height and direction that arise in traditional wave analyses that ignore wave interaction with strong tidal currents. Directional resolution of the ADP

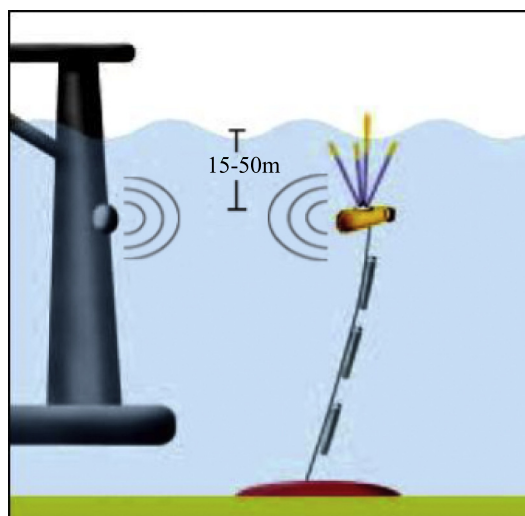


FIGURE 11.8 AWAC mounted on subsurface buoy. Real-time data telemetry is provided to the offshore structure via underwater acoustic modems. (*Source: Siegel, 2007, Ocean News & Technology, www.ocean-news.com.*)

wave spectra is improved; wave packets of similar frequency from different directions are distinguished. Because of its remote sampling capability and four acoustic beams, the RDI WorkHorse ADCPs can be deployed safely on the bottom yet act as a surface and near-surface array to measure waves.

Users of the RDI WorkHorse ADCP directional wave gauge can compare statistics from three independent data types measured simultaneously. The first data type is direct tracking of the water surface variation along each of the four beams. The second data type measured by the ADCP is wave orbital current fluctuations. These fluctuations are measured with each beam at 3–5 m depths near the water surface. Once these data are transformed to the surface using linear wave theory, the array has at least 12 elements spaced at longer beam-to-beam lags and shorter bin-to-bin lags. This combination produces wave-directional information across a wide bandwidth, including high-frequency waves in deeper water (e.g., measuring 4-s waves in 40 m of water). The third data type is obtained via a pressure sensor. The pressure sensor is used first to establish the depth of the ADCP below the sea surface, from which the separation of the ADCP array elements is determined. So the extra benefit of these pressure data is a third independent measurement of waves.

Wavelength is shortened when the phase speed of the wave is opposed by a background current. Consequent to this shortening is an enhanced decay with depth of the deep-water wave signature. Without including this influence in the data processing, the surface wave fluctuations inferred from pressure measurements at depth will be underestimated. Wave direction, too, can be distorted by wave-tidal flow interaction. Through the beam-former capability of the RDI WorkHorse ADCP directional wave gauge, the ADCP wave array resolves wave direction into 90 segments around the compass. The ADCP Directional Wave Gauge surpasses the traditional trade-off in wave gauge choices. The advantage comes from the ADCP's capability to measure remotely. In short, direct measurements of surface and near-surface variability are significant advantages compared with pressure-based wave gauges. For example, direct tracking of the surface increases the bandwidth of the wave gauge's frequency response. Whereas the frequency cut-off for the pressure-based wave gauge is about 5 seconds, the surface track ADCP detects periods shorter than 1.5 seconds. The ADCP measurements of wave orbital current fluctuations are near surface and have a high frequency cut-off near 2.5 s. By including the simultaneous current profiles in the wave analysis, the ADCP wave results do not suffer from biases in significant wave height and direction that arise in traditional wave analyses. There is also the improved directional resolution of the ADCP wave spectra,

distinguishing wave packets of similar frequency from different directions.

In summary, for situations where the performances of other wave gauges are limited, the ADCP Directional Wave Gauge continues to measure waves accurately. In particular, the ADCP has been demonstrated to have an impressive bandwidth from short local seas to long swells, eclipsing the performance of other common choices for wave gauges (Strong and Devine, 2000).

In addition to the application of ADPs for port operations and navigational safety, bottom-mounted, upward-looking ADPs have begun to be used for routine real-time reporting of current profiles in hazardous navigation channels (Froysa et al., 2007). For example, Aanderaa Data Instruments (AADI) of Bergen, Norway, installed a real-time environmental data observation station in the notoriously hazardous Bergen Fairway, which is the gateway to Bergen Port, on Norway's rugged West Coast. The majority of Bergen's maritime traffic must pass through these unfriendly straits, where complicated currents are driven by tides, storm surges, and wind. In January 2004 the motor ship *Rocknes* capsized in the straits with the loss of 18 lives, presumably by the force of strong currents and conflicting winds, causing the ship to strike an uncharted reef. The coastal observation station provides hitherto unavailable real-time graphical displays of oceanographic and meteorological data at all states of the tide, aided particularly by AADI's ADP.

Ocean current and surface wave data are measured by the RDGP 600 profiler, which is seabed-mounted in 22-m water depth within a gimbaled frame and cable-connected (75 m) to the host station. The unique feature of AADI's RDGP 600 profiling CM is its ability to measure current "bins" relative to both the sea surface and the seabed. The "relative to sea surface" current data ensures that measurements of current speeds are always available at critical "below surface" depths (e.g., ship's draught, irrespective of the state of the tide).

Acquired data are published to the Web. Results have shown that currents conflict at different depths and are additionally influenced by the prevailing wind conditions. The AADI coastal observation station has considerably improved the safety of vessels navigating this complex and hazardous waterway.

11.4. TRAWL-RESISTANT ADP BOTTOM MOUNTS

Uninterrupted data collection from areas of vigorous fishing activity is a very difficult task. In the areas with heavy trawling activities, a trawl-resistant seabed platform is usually used for protection of the ADP. ADPs' capability for high-resolution remote current profile measurements

has created new research opportunities in oceanography. This is especially true in shallow water, where instruments mounted on the bottom in trawl-resistant bottom mounts (TRBMs) can provide time series of current measurements with high vertical resolution from near surface to near bottom in water depths that include most of the world's continental shelves. Application of this technique was accelerated in the late 1990s by a new generation of ADPs that are smaller, lighter, and less expensive than their predecessors. Further encouraging the trend has been an increased concern for the ecological health of the oceans' shallow regions. At the same time, commercial and recreational use of near-shore waters is at a level that puts oceanographic equipment at high risk, especially for long-term deployments. TRBMs for such an application require careful engineering because a single high-value unit is exposed to a large number of risks, such as damage by trawlers, storms, corrosion, or bio-fouling.

Keeping the just mentioned requirements in view, Perkins et al. (2000) reported the development of a TRBM called *Barny* (so called because of its near barnacle-like shape) to meet the needs of long-term deployment of ADPs in water depths up to 300 m. The modified name *Barny Sentinel* is derived from a larger version developed several years ago at SACLANT Center and later extensively redesigned to incorporate an RDI Sentinel ADP and a Sea-Bird Wave-Tide Gauge. In this platform, a concrete ring surrounding the Fiberglas instrument housing serves as a ballast and impact protection. The ballast ring is made of concrete, reinforced with AISI316 stainless steel. This structure, like the rest of the Barny, is entirely nonmagnetic to prevent interference with the ADP compass. Barny's overall smooth profile minimizes the risk of being fouled by fishing gear.

The unit is lowered by electromechanical cable. Through this cable, real-time information regarding instrument pitch, roll, and depth is passed from a sending unit, which is temporarily attached during launch, to a PC-based display on the ship. In operation, two independent recovery modes may be activated by acoustic commands, one of which can operate whether or not the platform is upright. Once satisfactory placement on the bottom is confirmed, the external release is activated and comes away together with the sending unit. Two floats on the launch line provide buoyancy for the release. The acoustic releases also function as transponders so that bottom position of the platform can be determined acoustically. Features have also been included to facilitate recovery by remotely operated underwater vehicle (holes provided on the ballast ring permit recovery by this means). A series of tests and applications have validated all basic functions and trawl resistance. Platform cost has been kept below that of the onboard instruments while still maintaining the required high level of recoverability.

Skelin et al. (2008) reported two deployment configurations of trawl-resistant platforms for bottom-mounted ADPs. The "Light" deployment configuration is suitable in areas with no trawling activities. This configuration comprises an ADP, acoustic transponding release, lead weight with retrieving Kevlar rope mounted on the release, and two underwater buoyancies.

The "Heavy" deployment configuration with trawl-resistant seabed platform Mosor comprises an ADP, a battery canister for longer deployments, double acoustic transponding releases with adjacent buoyancies, and retrieving Kevlar rope. A trawl-resistant seabed platform protects the ADP and other equipment from the trawling nets due to polyester body slanted at typically 32°. This configuration is deployed with retractable inclinometer and remotely operated vehicle (ROV) to make sure that the trawl-resistant platform is set tightly to the seabed.

11.5. HORIZONTAL-FACING ADPs

There are many narrow straits in the world where tidal currents are strong. Most of them are of nautical importance, so real-time information of current velocity in the straits is required for the safety of navigation. In addition, the hydrodynamics of the very near-shore have been the subject of several decades of research for the simple reason that they have a large impact on the morphology and sediment transport on a daily scale. Morphology in this zone is far from uniform, and the formation (and destruction) of near-shore rhythmic patterns such as beach cusps, sandbars, erosion hotspots, and sand waves along the coast remains unclear to the present. Moreover, surf-zone currents play an important role in the transport of nutrients and bacteria in the coastal zone. From a beach tourism point of view, information on currents in the surf zone is of enormous importance to the safety of swimmers.

Precision measurements of currents are also required from the vicinity of offshore oil and natural gas production platforms. However, there are situations in which it is very difficult to measure water-current velocity in the center of a sailing route or in the vicinity of offshore production platforms by previously existing means. One of the reasons, especially pertaining to straits, is that strong currents and traffic congestion prevent placing an ADP on the seabed. Horizontal-looking ADPs capable of being side-mounted on bridges, canal walls, riverbanks, or other vertical structures in the coastal and offshore environments circumvent this difficulty. In horizontal-looking ADPs designed to meet these requirements, two transceivers, which are inclined to each other, are often employed so that the acoustic beams are divergent from each other. This scheme enables estimation of horizontal flow velocity vectors in sequential horizontal layers from the ADP.

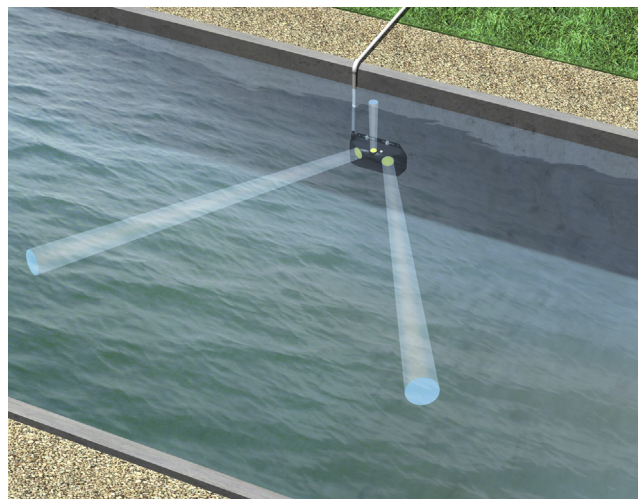


FIGURE 11.9 Pictorial view of a typical installation of a SonTek/YSI-make side-looking ADP on a wall, with an upward-looking transducer for wave measurement. The two acoustic beams are divergent from each other to enable estimation of horizontal flow velocity vector in sequential horizontal layers from the ADP. (Source: SonTek YSI Inc., www.sontek.com/pdf/news/newsrelease_apr07.pdf, reproduced with kind permission of Christina Iarossi, SonTek Marketing Communications, San Diego, CA 91921, USA.)

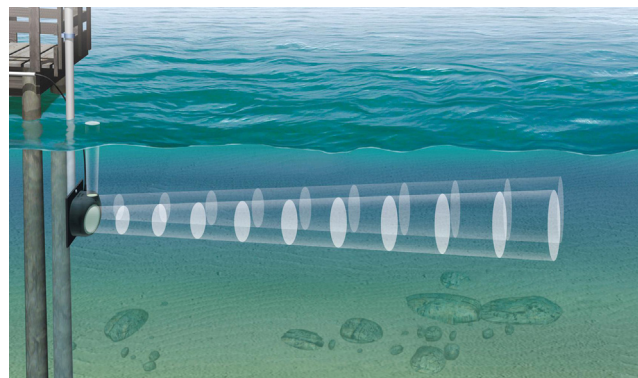


FIGURE 11.10 Side view of a typical installation of a SonTek/YSI-make side-looking ADP on a wall, with an upward-looking transducer for wave measurement. Successive bins in a horizontal layer of water columns are illustrated. Water-current measurement corresponding to each bin (radial current) in sequential layers is computed, and the horizontal flow velocities in sequential layers from various horizontal distances from the ADP are estimated using simultaneous radial current measurements from the respective bins of the two beams. (Source: SonTek YSI Inc., www.sontek.com/pdf/news/newsrelease_apr07.pdf, reproduced with kind permission of Christina Iarossi, SonTek Marketing Communications, San Diego, CA 91921, USA.)

Several manufacturers have produced different designs of horizontal-looking ADPs. A typical installation using a SonTek/YSI-make horizontal-looking ADP is illustrated in Figure 11.9. Because radial flow components are to be measured from various layers in the water column, the transceiver system is to be operated in a multiplexed mode, i.e., configuring it for transmission at one instance followed by reconfiguring it as a receiver before the backscattered signals have reached the transducer. In an incoherent system, each transceiver emits a stream of narrow-beam acoustic pulses, insonifying the water-borne scatterers along its path, and receives the Doppler-shifted back-scattered return echoes as the transmitted pulse continues its propagation through the water column. The duration of the pulse equals the gating time τ . The Doppler shift, as a function of time after transmission, yields the relative radial flow velocity as a function of the slant range in sequential layers at each of the “range-sliced” insonified volumes of the successive bins in a horizontal layer of water column (see Figure 11.10). The mean horizontal water-flow velocity vector at a given horizontal water layer, which is located away at a given distance from the ADP, is estimated from measurements of the two divergent radial flow components in this layer. Figure 11.11 provides the photograph of a more recent version of the Argonaut-SL family of SonTek/YSI-make side-looking ADP. Figure 11.12 provides an illustration of the scheme used for estimation of mean horizontal flow vectors in sequential horizontal layers of water using radial currents from these layers, which are

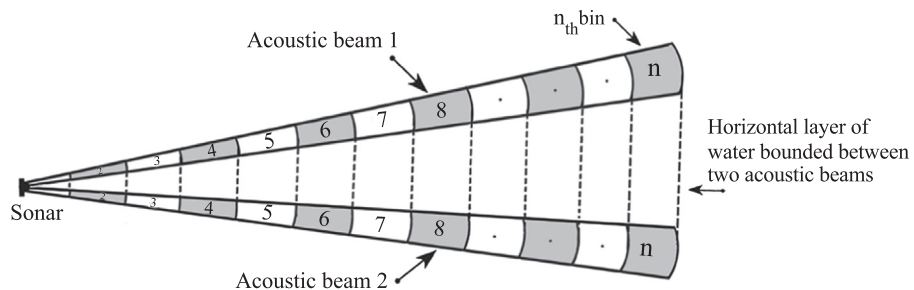


FIGURE 11.11 A more recent version of the Argonaut-SL family of SonTek/YSI-make side-looking ADP. (Source: Reproduced with kind permission of Christina Iarossi, SonTek Marketing Communications, San Diego, CA 91921, USA.)

bounded by two acoustic beams. Each measurement is an averaged value over a distance into the medium along the beam, expressed in terms of the two-way travel time. If a pulse of duration τ seconds, representing a time burst, is transmitted, the echo observation (integration) time must be equal to this duration. By adjusting the transmitted pulse length, the portion of the water column insonified at any given instant can be controlled and the desired range resolution can be achieved.

Teledyne RD Instruments Inc. launched its Horizontal ADCP (H-ADCP), which “looks” horizontally to distances

FIGURE 11.12 Illustration of the scheme used for estimation of mean horizontal flow vectors in sequential horizontal layers of water using radial currents from these layers, which are bounded by two acoustic beams.



of up to 200 m through the water to measure currents up to 5 m/s at up to 128 individual points (see Figure 11.13). Its applications include in rivers, where it monitors discharge rates and obtains horizontal profiles of water flow; in ports and harbors, where a pier-mounted instrument monitors shipping channels to aid navigation and safety; in estuaries, for defining complex circulation patterns and lateral mixing; on exploration rigs and seismic vessels; and in hydroelectric and tidal power plants.

The Teledyne RDI H-ADCP uses broadband signal processing. According to RDI, this enables it to obtain the best combination of range, resolution, and data quality compared with narrow-band solutions. The H-ADCP is self-contained and can be integrated with a telemetry module for relaying real-time information from remote sites.

Horizontal ADPs have begun to be employed recently in the surf zone, where it is very difficult to carry out water-current measurements by conventional means. Installation of instruments in this zone is not possible with boats due to the limited water depth. A horizontal ADP facing the cross-shore direction installed at low tide can provide a solution in these situations. Because the surf zone is relatively shallow, horizontal-looking ADPs with all beams aligned in a

horizontal plane are required to be used to prevent the acoustic beams from intersecting with the seafloor or the sea surface.

The first test of a horizontal ADP at a macro tidal beach in France showed promising results, especially for the mean flow velocities, revealing strong shear in flow in the vicinity of a rip channel. [de Schipper et al. \(2010\)](#) deployed a horizontal ADP (H-ADP) and a High Resolution upward-looking ADP (HR profiler) on a single measurement frame installed around 1 m below the low water line. The horizontal-looking ADP was a Nortek Aquadopp 600-kHz instrument, recording velocities in 9 bins along the beam axis with a bin size set at 5 m. The two transducer beams have a separation angle of 50° and a blanking distance of 0.5 m. Individual beams fan out with a total beam angle of 4°. The HR profiler was a Nortek Aquadopp HR 2000-kHz instrument. It was set up to measure in 44 bins of 1 cm in the upper part of the water column around high tide. The blanking distance was set at 10 cm. Its internal pressure sensor was used to record the water level above the instrument. Heading and tilt recordings allow examination of the motion of the ADPs.

Because the ADPs are in the very near shore, measurements are likely to be corrupted to some extent by bubbles and the instrument getting dry during low tide. Both instruments record the signal strength. Good velocity measurements are characterized by a high signal strength, which monotonously decreases in the bins further from the ADPs. Data having low signal strength are removed. Surf zone currents should be examined, taking into account the fact that the majority of these currents are induced by wave breaking and variations therein. Dissipation of wave energy generates strong currents of the order of 1 m/s in both cross- and alongshore directions. These wave-induced currents can be characterized by different time scales. Distinction can be made into four different time scales: (1) short-wave, high-frequency motion, (2) infra-gravity, low-frequency motion, (3) very-low frequency (VLF) motion, and (4) mean flow fluctuations. The perceived water-current motion in the surf zone is a superposition of all these elements.

The first category, the short-wave, high-frequency motions, has periods less than 25 s. These rapidly varying



Workhorse H-ADCP-600

FIGURE 11.13 Teledyne RD Instruments horizontal ADCP. (Source: Reproduced with kind permission from Margo Newcombe, Teledyne RD Instruments, USA.)

motions are governed by the orbital motion of individual waves. The next category, the infra-gravity, low-frequency motions, has periods in the range of 25 to 250 s. These infra-gravity motions are generated by the wave-height variations over time. High waves are often clustered in wave groups, and these wave groups are accompanied by infra-gravity waves (Longuet-Higgins and Stewart, 1962). Although the velocities and amplitudes of these infra-gravity waves are very little outside the surf zone (i.e., outside the wave-breaking zone), they become of greater relative importance inside the surf zone. The third category, very low-frequency (VLF) fluctuations, has wave periods in the range 250 s to 30 minutes. Water-motion velocity fluctuations with such large wave periods can be generated by instability of the along-shore current-induced or wave-group-induced surf zone eddies (MacMahan et al., 2010). These slow motions have been hypothesized to be important for the initiation or development of near-shore rhythmic patterns (Reniers et al., 2004) as well as the exchange of transported material between the surf zone and the inner shelf (Reniers et al., 2009). The magnitude of VLF velocities and especially the surf zone eddies is influenced by the characteristics of the wave field (i.e., wave period, directional and frequency spreading). The fourth category is the mean flow fluctuations with wave periods larger than 30 minutes. This flow pattern is typically governed by tidal currents.

Based on the just-mentioned considerations of the inner and outer surf zone water-motion characteristics, de Schipper et al. (2010) “dissected” their horizontal and vertical ADP measurements in the very near shore at the Dutch coast in the North Sea. Measurements of both instruments showed the presence of substantial VLF oscillations on one of the field days. The observed root-mean-squared velocity of the oscillations in the VLF frequencies ($30\text{ min} > T > 250\text{ s}$) was 0.31 m/s, which is substantial compared with that of the short-wave motion. This finding implies that the VLF oscillations are not only reserved to ocean coasts with medium to high period ($T > 10\text{ s}$) waves. de Schipper et al. (2010) found that a horizontal-looking ADP is most valuable when deployed outside the surf zone, where (1) the flow is more uniform, and (2) the beams intersect less with the sea surface or the seafloor.

In any commercial system, size and weight matter greatly in view of easier transportation and installation in wider, deeper environments. Thus, the design considerations have often resulted from a good deal of customer input on how the products are used. In particular, ergonomic features are likely to open up more applications and thus save on installation and maintenance time.

A limitation of the previously mentioned two-beam system is the requirement to make an assumption that the flow field in the horizontal water layer bounded between the two horizontal beams is uniform. This assumption need not necessarily be true if there are abrupt

depth discontinuities below this layer or if the water channel is of nonuniform width. To overcome the difficulty of real-time measurements using bottom-mounted ADPs and simultaneously circumvent the limitation of two-beam geometry, the Hydrographic Department and the Japan Hydrographic Association developed a new side-looking H-ADP (Sato et al., 1999) for measuring water-current speed and direction in the center of a narrow strait by transmitting acoustic pulses along a horizontal plane and receiving the echoes at the coastline. The main purpose of the development was to measure strong currents in narrow channels such as the Kanmon Strait in Japan, which is an important sailing route connecting the Sea of Japan and the Seto Inland Sea, which many vessels pass through. The ADP is designed to be placed on a vertical wall beneath the sea surface.

The Horizontal ADP operates by transmitting very narrow acoustic beams horizontally from only one transducer. The beams are transmitted in seven directions, one after another. The angle between successive beams is 10° and the interval of transmission is a second, so that it takes 7 s to transmit beams in seven directions. A single acoustic beam measures a single water-flow velocity component, which is the component parallel to the beam. Radial currents measured by two neighboring divergent beams, which are at an azimuthal separation of 10° , are used to compute the vectorial mean horizontal velocity within the water layer bounded between these two beams. The seven acoustic beams provide the horizontal profile of the water-current velocity in a fan-shaped horizontal plane every 7 s.

When horizontal beams are to be transmitted in shallow water, it is necessary that the beams be of narrow width. If the beam is wide, the echoes from the surface or the bottom are likely to return to the transducer simultaneously with the echoes from the target distances. Sato et al. (1999) generated the required narrow beam using an array of 6,912 elements (144 vertically \times 48 horizontally) in the acoustic transducer. The cell size is 10 to 99 m. The transducer’s axis must be located more than 5 m below the sea surface so as to measure the surface currents.

The Horizontal ADP consists of four parts: transducer, amplifier, signal processor, and data processor. The amplifier forms the beams and amplifies the signals. The signal processor detects the Doppler frequency shifts and computes the horizontal water-flow velocity components. The data processor displays the distribution of horizontal water-current speed and direction. The transducer was rigidly fixed on an iron frame and mounted on the side wall of the quay by a crane.

Sato et al. (1999) deployed and field-tested the Horizontal ADP at the Kanmon Strait in Japan, which is an important sailing route connecting the Sea of Japan and the Seto Inland Sea. The length of the strait is about 10 km and its width varies from 500 m to 2 km. More than 700 vessels

pass through the Kanmon strait every day. The maximum tidal current in this strait reaches about 5 m/s at the narrowest region. The depth at the quay is about 12 m, and the transducer was set at 5 m below the chart datum (CD) level. Water-current speed is expressed in color, and current direction is shown by an arrow. The center of the sailing route is about 500 m away from the quay. Field tests carried out by Sato et al. confirmed that current speed and direction within 500 m of the transducer can be measured by this new ADP. Analysis of the measured data revealed that the phases of the two most dominant harmonic constants of M2 (principal lunar semidiurnal tidal current) and K1 (lunisolar diurnal tidal current) propagate from the coastline to the sailing route, with amplitudes increasing toward the center of the channel. According to Sato et al. (1999), this observation agrees with the theory of the tidal current in a channel.

11.6. SUBSURFACE MOORED ADPs

Dissemination of tide and tidal current predictions is a critical part of several maritime nations' efforts toward promoting safe navigation in their waterways. To assure that the tidal current predictions are reliable, new observational data must be collected periodically, requiring a variety of CM platforms suitable for different environments. For example, the Center for Operational Oceanographic Products and Services (CO-OPS) of NOAA's Ocean Service (NOS) manages a Current Observation Program (Earwaker and Zervas, 1999) with a main objective of improving the quality and accuracy of the annually published Tidal Current Tables (NOS, 2001). For this purpose, CO-OPS strives to use off-the-shelf technologies,

when possible, to help reduce costs and improve efficiency of field operations. Alternative platforms to the commonly used bottom-mounted platforms are subsurface mooring buoys of various shapes (e.g., spherical; streamlined).

Notwithstanding excellent performance of any oceanographic instrument under laboratory conditions, it is necessary to examine its performance under the field environments where it will be deployed. Taking this requirement into account, Bourgerie et al. (2002) carried out several field experiments at the mouth of the Delaware Bay, which is relatively deep (45 m) and the currents there are fairly strong (> 100 cm/s). The bottom-mounted and the subsurface buoy-mounted ADPs used for the experiments (RDI Workhorse Sentinel, WH-300; see Figure 11.14) transmit sound pulses along four narrow beams. The platform was a subsurface, torpedo-shaped, streamlined buoy (SUBS), which was developed and field-tested at the Bedford Institute of Oceanography (Hamilton et al., 1997). This buoy is relatively lightweight (just under 40 kg with ADP) and is considerably easier to handle than the 350-kg bottom-mounted platforms typically used for current observation programs. Use of a streamlined buoy in place of a spherical buoy effectively reduces drag and greatly reduces mooring vibration induced by vortex shedding (Hamilton, 1989). The test consisted of analyses of pressure, tilts, and heading of the subsurface, moored, upward-looking ADP to determine how well its platform performs in high flows. The dynamics of the SUBS were determined from the ADP's pressure sensor, tilt sensors, and compass. It was found that the buoy's tilts fluctuated regularly with the reversing tidal current; the pitch ranged from 0 to -6° , and the roll ranged from -3 to -6° . Although the roll of the SUBS improved with increased current speeds, the pitch of the



FIGURE 11.14 Teledyne RD Instruments Workhorse Sentinel. (Source: Reproduced with kind permission from Margo Newcombe, Teledyne RD Instruments, USA.)

SUBS became larger at higher speeds. However, these tilts are internally corrected by the ADP and are well within acceptable limits.

There are field-specific issues for which no internal corrections are practical. For example, the water current applies a force along the entire mooring length, causing the mooring to incline and lowering the SUBS down in the water column. This vertical displacement is an important factor in analyzing and interpreting the current velocity profile data. If the SUBS is regularly displaced beyond the cell size, the mapping of the cell depths becomes overly complicated.

The vertical displacement can be isolated from the ADP's pressure sensor measurements by removing the tidal signal observed at a nearby sea-level gauge. Assuming a small time lag between the two locations and referencing both measurements to the same datum (e.g., mean lowest low-water level), the water levels at the sea-level gauge station can be subtracted from the pressure-sensor-derived water-level measurements to arrive at a value referred to as ΔH . The ΔH values represent the distance from the pressure sensor to the water surface minus the tidal elevation; therefore, the ΔH values approximate the vertical movements of the buoy. Accumulation of sediments within the cavities of the SUBS and settling of the anchor into bottom sediments have been offered as two possible explanations for the observed vertical shift of the subsurface buoy (Bourgerie et al., 2002). A reference level from which to quantify vertical displacement due strictly to the current can be derived by averaging all of the ΔH values occurring at slack water (speeds less than 5 cm/s), after the anchor had settled into bottom sediments. Subtraction of this average from all ΔH values yields the vertical displacement of the SUBS.

During slack water, the buoy remains relatively stable in the vertical, but it is suppressed downward with increasing current speed. It was found that the flood currents at the experimental site (Delaware Bay) had a greater effect on the mooring, causing a lowering of the SUBS by as much as 1.9 m. The slightly weaker ebbs produced a maximum vertical displacement of 0.6 m. The flood currents consistently caused a relatively larger vertical displacement of the buoy than the ebb currents.

The amplitudes and phases for six of the largest tidal current constituents (comprising more than 93 percent of the total current) obtained from time-series measurements of SUBS-borne and bottom-mounted ADPs and subjected to similar post-processing and quality-control procedures, showed minor differences. The differences seen in the amplitudes and phases of the two datasets have been attributed in part to a changing water-density structure of the Bay and other seasonal changes in water conditions and flow over the course of the year. (The reference bottom-mounted ADP observations were collected in the summer, whereas the SUBS-borne ADP observations were collected

in the winter.) Tidal current predictions for the 33 days of the SUBS-borne ADP measurement period, generated from each set of 24 constituents (SUBS-borne and bottom-mounted ADPs), yielded good agreement between all three series over a representative period of time. Based on tidal current predictions for 34 days, SUBS-derived tidal current predictions seemed to slightly underestimate the current near maximum flood. However, the overall RMS of the residual current (bottom-mounted ADP observations – SUBS predicted) was 15.3 cm/s, which has been stated to be within the typical range of values seen for flows of this magnitude.

Analyses such as these permitted assessing the quality of subsurface deployed ADP current measurements against those made from stable, bottom-mounted platform. It is seen that there is a certain degree of data degradation due to subsurface mooring dynamics. Bourgerie et al. (2002) exposed the SUBS-borne ADP mooring to maximum current speeds of approximately 120 cm/s. At speeds of this magnitude, the mooring angle was found to be steep and vertical displacement approached 2.0 m. Many areas in the world oceans have significantly stronger currents than those observed at the mouth of the Delaware Bay; hence the subsurface buoy may not be a suitable platform for these locations.

There are four major set-up parameters for moored ADPs: deployment depth, space between measurements in depth and time, data averaging, and deployment duration. These parameters can be modified via professional software, which ADP manufacturers provide. Professional software for deployment planning shows the consequences of set-up choices in terms of power consumption, memory requirements, and velocity precision. For optimizing ADP setup, the importance of the three parameters from the so-called *trade-off triangle* is crucial. These parameters are range, resolution, and random noise (Skelin et al., 2008). Range is associated with transmission frequency. Lower frequency results in longer profiling range. Doubling the cell size will inject two times more acoustic energy into the sea. Usually, profiling range is enhanced by colder and fresher water. Smaller cell size will provide finer resolution but lesser profiling range and more random noise. Therefore, ADP will require a larger measuring period. Doubling the number of cells doubles the power consumption and the random noise. Broader bandwidth and lower frequency will provide finer resolution. More dynamic motions and more turbulence will increase the random noise. More suspended material in the sea will provide lower noise as a result of enhanced echo intensity and, therefore, will improve velocity precision.

Schott (1986) located an ADP at depths of 470 and 610 m on subsurface mooring lines deployed in the Florida Current and obtained detailed vertical profiles over five days.

11.7. DOWNWARD-FACING SHIPBOARD ADPs

Strong ocean currents can disrupt various deep-water activities and cause downtime for several commercial activities such as hydrocarbon exploration and production activities. Thus, accurate and timely observations can help with planning and assuring safe operations. Remote sensing cannot always be counted on to provide timely observations of the sea surface away from the coast. Drifting buoys have proven to be a cost-effective means of collecting ocean current observations; however, drifters report only near-surface currents and the Lagrangian techniques cannot target and monitor a specific site or area. ADPs mounted on moorings and offshore platforms can provide real-time current-flow information but are not always optimally located. ADPs deployed on ships provide a viable way to survey ocean-current profiles in a specific region of interest. Low-frequency ADPs operating at 38 kHz or 75 kHz are needed to provide synoptic coverage of the ocean-flow features from relatively deep-sea regions. Low-frequency operation demands large ADPs, which have to be hull-mounted systems mostly deployed on research vessels.

The development of shipboard ADPs—a logical extension from Doppler navigation systems, which operate on the signals returned from the seabed—began in the 1980s, and a number of successful applications of the technique have since been described in the literature. Surveys using shipboard profilers provide detailed information about the spatial structure of currents in a way that cannot be matched by moored instrument arrays. Such systems were expected to provide a powerful tool in large-scale international campaigns such as the World Ocean Circulation Experiment (WOCE), particularly if they could be made suitable for use on ships of opportunity (Cutchin et al., 1986).

Shipboard hull-mounted ADP systems are found in two geometric configurations: three- or four-beam systems. In a typical three-beam system, the beams are spaced 120° apart in the azimuth, and each beam points down at an angle of ϕ ° from the vertical. One beam (say, beam 1) is generally oriented forward along the ship's longitudinal axis, and the other two beams (say, beams 2 and 3) lie along the port and starboard quarters (see Figure 11.15). Based on

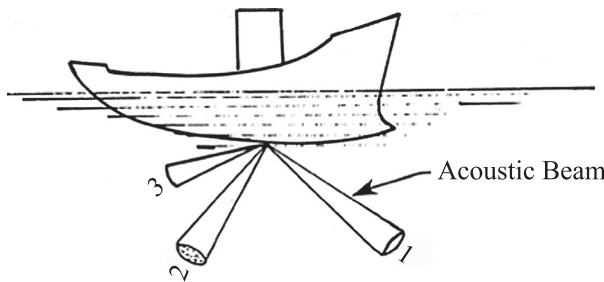


FIGURE 11.15 Geometry for a hull-mounted three-beam ADP.

this geometry, the along-track and the cross-track relative velocity components at various depth layers may be estimated in terms of the in-beam (i.e., radial) Doppler shifts for the three beams from the corresponding depth layers. The mean relative horizontal flow velocity vector may be considered to consist of a horizontal flow component (say, V_y) along the longitudinal axis of the ship (i.e., along the ship's direction of motion) and an orthogonal horizontal flow component, say, V_x . These components are given by the relation (Theriault, 1986a):

$$V_y = \left(\frac{c}{6\omega \sin \phi} \right) (\omega_{D(2)} + \omega_{D(3)} - 2\omega_{D(1)}) \quad (11.11)$$

$$V_x = \left(\frac{c}{2\sqrt{3}\omega \sin \phi} \right) (\omega_{D(3)} - \omega_{D(2)}) \quad (11.12)$$

where c is the velocity of sound in water, ω is the transmission frequency in angular notation, ϕ is the angle (in degrees) made by each beam from the vertical, and $\omega_{D(1)}$, $\omega_{D(2)}$, and $\omega_{D(3)}$ are the Doppler shifts (in angular notation) measured by the beams 1, 2, and 3, respectively. Because only three components of velocity are present, i.e., two horizontal and one vertical component, only three beams are sufficient in principle to fully describe the flow field. However, if the beams are more than three, the performance of the profiler correspondingly increases. For example, in the three-beam system just mentioned, the along-track horizontal flow component V_y is coupled to the Doppler shifts from all the three beams (see Equation 11.11). Furthermore, lack of a coplanar companion beam makes the three-beam system sensitive to pitch and roll of the vessel.

To circumvent some of the limitations inherent in a three-beam Doppler profiler system, a four-beam system has been introduced. This system employs two “Janus configurations” consisting of a total of four beams oriented 90° apart in the azimuth, each beam making an angle of ϕ ° to the axis of symmetry of the transducer system (see Figure 11.16).

Joyce et al. (1982) described a pulsed, 300-kHz, four-beam, hull-mounted acoustic transducer, which was used to obtain vertical profiles of upper ocean currents relative to a ship (*R. V. Oceanus*), the lateral motion of which was determined by changes in LORAN-C position. The

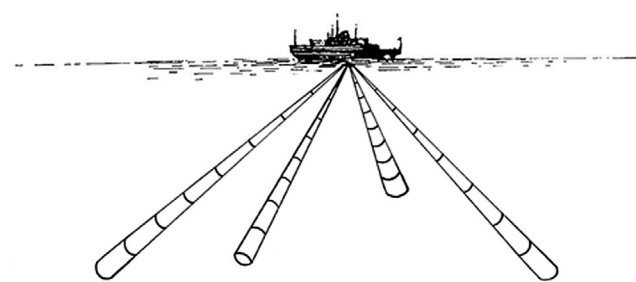


FIGURE 11.16 Geometry of a hull-mounted four-beam ADP.

acoustic transducer and current-profiling electronics were produced by Ametek-Straza (Rowe and Young, 1979) and were successfully used in the western North Atlantic.

The acoustic profiling system consisted of two main parts: the Ametek-Straza Doppler current profiler and a controller-data logger built at the Woods Hole Oceanographic Institution. In this system, a 300-kHz acoustic pulse is transmitted from a transducer mounted in the hull of the ship in four beams down through the water column. As the acoustic signal travels through the seawater, it is scattered by small particles, temperature microstructure, or turbulence. By measuring the frequency of the return signal as a function of time or, equivalently, acoustic range, a profile of water velocity along the acoustic path can be obtained. Combining the data from the four beams with the ship's heading and subtracting the ship's translation over the Earth from navigational data yield a vertical profile of ocean currents.

In this measurement, a 254-cm-diameter transducer assembly had four 10-cm-diameter flat-plane acoustic radiators-receivers mounted at 30° angles to the vertical; two pairs of transducers defined two orthogonal vertical planes. Each radiator transmitted a 3° conical beam at 300 kHz. The beams could be approximately aligned in the fore, aft, port, and starboard directions relative to the ship. The four radiators were driven from one common 40-W power amplifier that produced a sound pressure level of +225 db relative to 1 µPa at a distance of 1 m along each beam. Preamplifiers mounted in the transducer assembly amplified the return signals and sent them via a shielded multi-conductor cable to a second set of amplifiers before the signal processing stage. The transducer assembly also included a thermistor temperature sensor to measure seawater temperature to compensate for sound-speed variations due to temperature fluctuations.

Pulses of 300-kHz sound of 10 or 20 ms duration (pings) were emitted at regular intervals from the four radiators. The returned signal was detected by the Ametek-Straza electronics. Following transmission of an acoustic pulse, the returned, amplified signal was detected in a frequency-locked loop, the frequency of which was measured in each of 31 time intervals. These intervals were switch-selectable for 5 or 10 m corresponding to vertical depth bins of 3.2 or 6.4 m, allowing for the 30° beam angles from the vertical. The signal processor measured the amplitude of the return signal and set a quality flag for each Doppler determination in which the signal strength was too low. Profile repetition was once every 1.2 s. The signal processors converted each good Doppler count to a 12-bit binary data word and a good-bad status bit for each depth bin of each beam. Resolution of Doppler-induced currents for a single ping was 1.2 or 2.4 cm/s, depending on the averaging time of 10 or 5 ms in the frequency-locked loop. A more detailed discussion of the detection electronics is given by Rowe and Young (1979).

To record information about the ship's heading and navigation, interface modules were built to convert data from the ship's gyrocompass, a Northstar 6000 LORAN-C receiver, and a Magnavox 706 satellite navigation receiver into a serial datastream that was transmitted over a 20-mA current loop. Each module was assigned a unique address and responded when the data controller sent out the proper address code. The current loop was selected because it required only two simple wires to connect modules located at various places on the ship. It also had a high level of noise immunity. Typically, this serial ASCII information loop (SAIL) transmits data at a rate of 2,400 bits per second (bps).

If flow homogeneity is assumed at a given horizontal plane bounded by the radial bins of the acoustic beams at that horizontal plane, the horizontal flow component u and the vertical flow component w at a given depth bin in a forward-aft-looking Janus arrangement are given by (Joyce et al., 1982):

$$u = \left(\frac{\Delta\sigma_1 - \Delta\sigma_2}{4\sigma} \right) \left(\frac{c}{\sin\phi} \right) \quad (11.13)$$

$$w = \left(\frac{\Delta\sigma_1 + \Delta\sigma_2}{4\sigma} \right) \left(\frac{c}{\cos\phi} \right) \quad (11.14)$$

where $\Delta\sigma_1$ and $\Delta\sigma_2$ are the Doppler shifts measured by beams 1 and 2, respectively, in the forward-aft-looking Janus arrangement corresponding to a given horizontal plane bounded by the respective radial bins; σ is the acoustic frequency; c is the sound speed in the seawater medium; and ϕ is the angle made by the forward-aft-looking beams 1 and 2. Since the same argument can be made with the orthogonal pair of beams 3 and 4, the horizontal velocity vector can be estimated along with two independent estimates of the vertical velocity. The difference in the two vertical velocities is therefore related to acoustic noise, imperfect estimation of Doppler shift, and spatially variable currents.

Near the ocean surface, the particle motions due to surface waves are greater, but the physical separation of the two ensonified regions is less. Therefore it is not obvious which of these factors dominates at any depth. Unlike the stable platform *Flip*, ship motion due to surface waves is a significant signal in the Doppler returns and must be considered. The instantaneous decomposition into fore, aft, and athwartship velocities must be put into geographical coordinates because the ship is yawing as it pitches, heaves, and rolls. This is done by measuring the ship's heading for each data cycle. One method of reducing the error induced by ship motion is to vector-average the Doppler currents over many wave cycles and estimate lateral ship velocities from LORAN-C data. However, the resolution of LORAN-C is usually insufficient to detect subtle changes

in ship speed. Thus, wave-induced noise will be present, but it will be reduced by averaging over many wave cycles.

ADPs are mounted on moving vessels to map the vertical profiles of upper ocean horizontal currents, but the measured relative velocity profiles (with respect to the velocity of the vessel) can be transformed into an absolute velocity profile using the ship's speed and heading information for each data cycle. In locations where good LORAN-C coverage is available, the vessel's lateral motions can be determined by measurements of changes in LORAN-C position within an uncertainty of 5 to 10 cm/s. This data can, in turn, be used to correct the inherent errors that tend to creep into the velocity field map as a result of the ship's lateral motion during measurements of velocity profiles (Joyce et al., 1982). When both the LORAN-C and the Doppler profiler data are suitably filtered, the resultant absolute velocity profiles are estimated to be accurate to within ± 2 cm/s (Trump et al., 1985). Although this procedure cannot remove the wave-induced noise, these errors can be reduced to a certain extent by vector-averaging the measurements over many wave cycles.

As mentioned earlier, when mounted beneath a vessel, the system is generally operated with one pair of mutually diverging beams (say, beams 1 and 2) oriented along the longitudinal axis of the ship and the other pair of beams (say, beams 3 and 4) oriented along an orthogonal plane so that the profiler resolves the relative velocity field at any given depth layer into along-track and cross-track components. If $\omega_{D(1)}$, $\omega_{D(2)}$, $\omega_{D(3)}$, and $\omega_{D(4)}$ are the Doppler shifts measured along the beams 1, 2, 3, and 4, respectively, the relative horizontal flow component V_y along the longitudinal axis of the ship is given by the relation (Theriault, 1986a):

$$V_y = \left(\frac{c}{4\omega \sin\phi} \right) (\omega_{D(1)} - \omega_{D(2)}) \quad (11.15)$$

and the relative horizontal flow component V_x perpendicular to the longitudinal axis of the ship is given by:

$$V_x = \left(\frac{c}{4\omega \sin\phi} \right) (\omega_{D(3)} - \omega_{D(4)}) \quad (11.16)$$

The sign of ω_D depends on the direction of flow relative to the respective axis of the transducer system. In this four-beam geometry, each horizontal flow component is estimated as a mean of the Doppler shifts from the two symmetrically oriented beams in each of the Janus configurations in the two mutually orthogonal vertical planes. It is thus evident that, in the four-beam geometry, the Janus configuration tends to minimize the sensitivity to pitch and roll of the vessel. In addition to these obvious differences in performance, statistical analysis by Theriault (1986b) suggests that, for similar operating conditions, the four-beam geometry yields an enhanced performance

compared to that of the three-beam system. Despite the limit on the maximum allowable ship speed (Theriault, 1986b), the ship-mounted ADPs possess a remarkable feature of large spatial coverage.

Joyce et al. (1982) succeeded in measuring the upper 100-m layer of the Gulf Stream along a traverse line of length about 200 km with an ADP mounted on a ship hull. Vertical profiles of horizontal currents for three selected 10-min segments (see arrows in Figure 11.17) show the change in vertical structure across the section (see Figure 11.18).

Gawarkiewicz et al. (2004) have reported shipboard ADP measurements from the northern half of the South China Sea. Whereas geostrophic calculations from individual sections gave extremely poor results due to aliasing of both tides and high-frequency motions, the ADP measurements were found to be in agreement with the anticyclonic winter circulation in the measurement region from numerical model calculations.

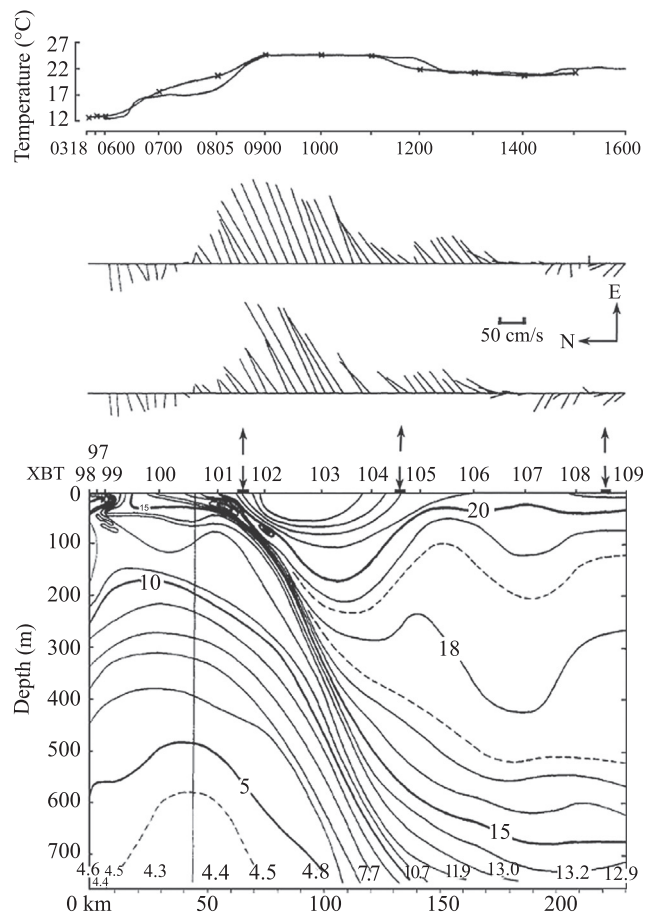


FIGURE 11.17 Section across the Gulf Stream showing thermistor and bucket temperatures (note the 30-min lag of the thermistor). Upper panel: Vector-averaged currents at depths of 28 and 99 m (second and third panels, respectively). XBT section with XBT numbers and three 10-min segments selected for current profiles and denoted by the arrows. (Source: Joyce et al., 1982.)

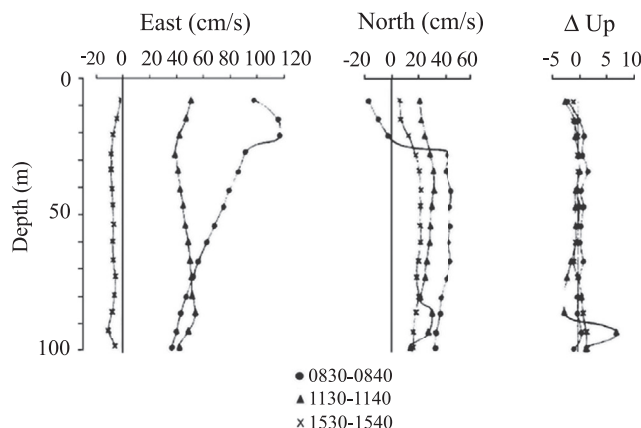


FIGURE 11.18 Vector-averaged horizontal velocities for three 10-min time intervals shown in Figure 12.19 from the Gulf Stream north wall (●), south wall (△), and Sargasso Sea (x). Difference between two vertical velocity estimates is plotted at the right on an expanded scale. Only data judged “good” by Ametek-Straza interface cards were used. The large shear at 20 m in the north wall profile is across the base of the mixed layer and could be due to inertial waves. (Source: Joyce et al., 1982.)

11.8. TOWED ADPs

As indicated earlier, vessel-mounted ADPs have become a standard tool on many research vessels for horizontal and vertical current profile measurements. Their operation has been studied by Kosro (1985), Didden (1987), Chereskin et al. (1987), and Joyce (1989). However, beyond the limitations inherent in the ADP system itself, some limitations have been identified with vessel-mounted systems (Chereskin et al., 1989; Chereskin and Harding, 1993). For example, vessel-mounted ADP systems utilize the ship’s inertial or gyro compass. A misalignment generally exists between the reference direction used by the ADP and that of the ship’s gyro. Joyce (1989) details a calibration routine to determine this constant misalignment. Pollard and Reed (1989) found that abrupt changes of the ship’s course cause yet another compass error as the turn excites persistent Schuler oscillations at periods of 20 and 80 min that bias the compass readings. Although a calibration routine can resolve the misalignment problem, no recourse is available for the Schuler oscillations, the amplitude of which can reach several degrees.

Entrainment of air bubbles is another issue. Air bubbles near the transducer heads and compass biases often degrade shipboard ADP observations (King and Cooper, 1993). New (1992) reported that as the ship heaves, a cloud of air bubbles entrain under the hull of the ship. The bubble cloud then sweeps past the transducer heads in a layer about 1 m thick. This layer degrades ADP current estimation because air bubbles have different acoustic properties than the seawater below. New (1992) found, however, that the problem can be overcome when the transducer heads extend 1.5 m beneath the hull of the ship. Thus, in the use of

vessel-mounted ADP systems, utmost care needs to be taken to ensure that they operate in a low-noise and bubble-free environment.

Probable solutions to overcome the problems related to the hull-mounted ADPs might be to deploy the ADP over the side of the ship or tow the ADP. Low-frequency ADPs are required to profile currents over a large depth extent; therefore, such ADPs would necessarily be large in size. However, deploying a large ADP over the side of a ship would require a large mounting system to be welded to the vessel to withstand structural loading while underway. Thus, it requires modification of the deployment vessel hull. In addition, it would be difficult to design a mount that would position the transducer head deep enough and isolated enough to assure a quiet, bubble-free environment.

A completely submerged, towed ADP system cannot entrain bubbles. In addition, it exhibits neither the Schuler oscillation problem nor the direction misalignment problem because it generally relies on a magnetic compass. The ship’s hull and the tow platform, however, may induce magnetic variations that can be large and must be removed through a calibration routine. Hence, both ship-mounted and towed ADP systems require careful *in situ* calibration to account for compass biases. Taking all these into account, it is considered that towed ADPs offer an attractive alternative to vessel-mounted ADPs.

There are other relative benefits in the use of a submerged towed system. A towed system can be used from ships of opportunity, allows easy maintenance, and is expected to provide remedies to several problems of vessel-mounted systems. Kaneko and Koterayama (1988) first introduced a towed ADP. They mounted a 150-kHz ADP (RD Instruments RD-SC0150) on a fish (sled) made of fiber-reinforced plastic (see Figure 11.19), and the sled/fish

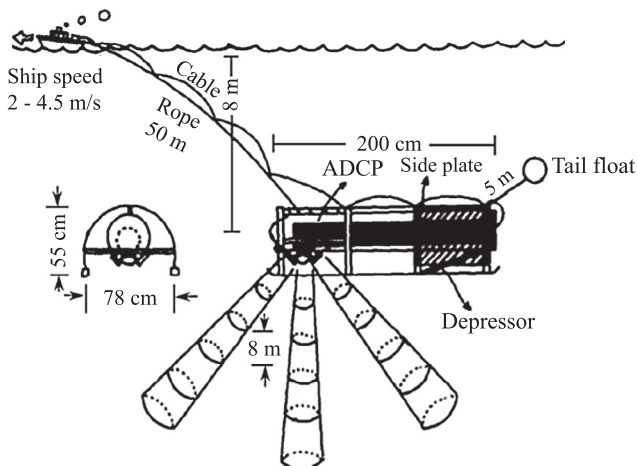


FIGURE 11.19 Schematic diagram of the fish-mounted ADCP system. The ADCP, located inside the cylindrical fish body, is shown in solid black. The hatched region indicates the location of the side plates. On the left is a front view of the fish. (Source: Kaneko and Koterayama, 1988.)

was towed with a 50-m-long nylon rope behind a research ship. The nylon rope is expected to dampen the direct response of the fish to ship motion. When the ship was on station, the ADP fish floated up to just below the sea surface because of the buoyancy of a tail float. The trailing buoy also stabilized the fish, much as a tail stabilizes a kite. At ship speeds of 2.0–4.5 m/s, the fish was designed to be submerged up to a constant depth of 6–8 m beneath the sea surface by the downward lift force acting on a depressor.

The front portion of the fish was rounded to reduce hydrodynamic forces. The geometrical positions of the towed rope and the depressor were carefully selected to stabilize fish motions. In particular, the tail float and the side plates served to suppress the yaw and roll motions of the fish. During the traverse survey, the fish could not be turned over because of the heavy transducers and the tail float. A flux-gate compass and dual-tilt sensors located inside the ADP transducer housing were used to convert the measured flow velocities from the instrument coordinates to Earth coordinates (north, east, and vertical velocity components). The ADP fish was covered by thin stainless frames to protect it from collision with the ship's hull during deployment and recovery.

Power to the ADP was supplied from the ship through a cable that also contained wires for an RS-422 serial link. The cable was loosely tied to the nylon rope. Internal ADP sensors measured the heading, pitch, and roll of the sled. Four transducers were arranged in a downward-facing Janus configuration. Water temperature was also measured with a thermistor placed in a space between the ADP transducers. The ADP transmitted 10.6-ms acoustic pulses every 1.8 s. The 10.6-ms pulse width corresponds to a depth resolution of 8 m. The measured data were transferred automatically to an onboard microcomputer through the cable.

Unlike the conventional ship-mounted ADP, the fish-mounted ADP is expected to exhibit the following benefits (Kaneko and Koterayama, 1988):

- Ocean currents are accurately measured, even under severe sea surface conditions.
- Cavitation noises generated by the ship's propeller are much reduced around the fish.
- Interference problems caused by bubbles entrained under the ship's hull do not occur for the fish.
- The fish-mounted ADP can be operated from any unspecified research ships.

Keeping ship speed and heading smooth and constant serves to improve the accuracy of observation. Fish motions measured by the flux-gate compass and the dual-tilt sensors over the whole traverse survey are shown in Figure 11.20. Kaneko et al. (1990) found that when the water depth was shallower than 480 m, the ADP was able to track the sea bottom to obtain fish speed relative to the

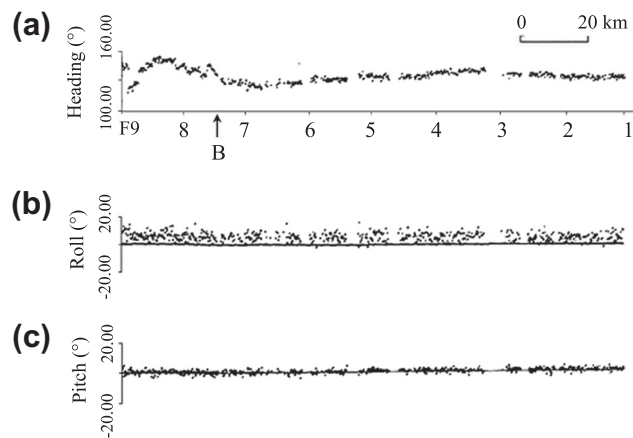


FIGURE 11.20 Fish motions measured by the flux-gate compass and the dual-tilt sensors over the whole traverse survey. (a) Heading. (b) Roll angle. (c) Pitch angle. (Source: Kaneko et al., 1990.)

bottom. They also found that when the bottom is within range of the ADP, there is a near-bottom layer in which good data cannot be obtained. This limitation of ADP measurements is caused by transducer side lobes reflecting directly from the bottom. Kaneko et al. (1990) obtained detailed velocity measurements of the Kuroshio Current with their sled-mounted, towed ADP system. The vector time series (stick diagrams) of the Kuroshio current velocities obtained from the ADP measurement are shown in Figure 11.21, with the time plot of water temperature obtained from the thermistor. The Kuroshio Current exhibits a profile like a jet flow, with a width of about 80 km and the maximum current of about 1.3 m/s at the center of the jet (near the middle of the transect) near the surface. The dominant direction of the current was northeastward. The current velocity decreased slowly with depth; it was near 1.0 m/s at 400 m depth. Based on these measurements, Kaneko et al. (1990) concluded that the magnitude of the Kuroshio Current in this region is significantly underestimated through conventional geostrophic calculations that use a level of no motion at 700 or 800 m depth. It was also concluded that there are many similarities between the Florida Current (flowing between Florida and the Bahamas) and the Kuroshio Current (flowing between the East China Sea shelf edge and the Ryukyu Islands). Therefore, many of the mechanisms of these two current systems should be the same.

Towed ADP systems have undergone several design modifications with a view to improving their performance. For example, Munchow et al. (1995) reported a towed ADP platform, which contains both an upward- and a downward-facing ADP (see Figure 11.22). This system differs in design, construction, and operation from that of Kaneko and Koterayama (1988) and Kaneko et al. (1993). The towed fish reported by Munchow et al. (1995) consists of a hydrodynamic body, a seven-conductor torque-balanced

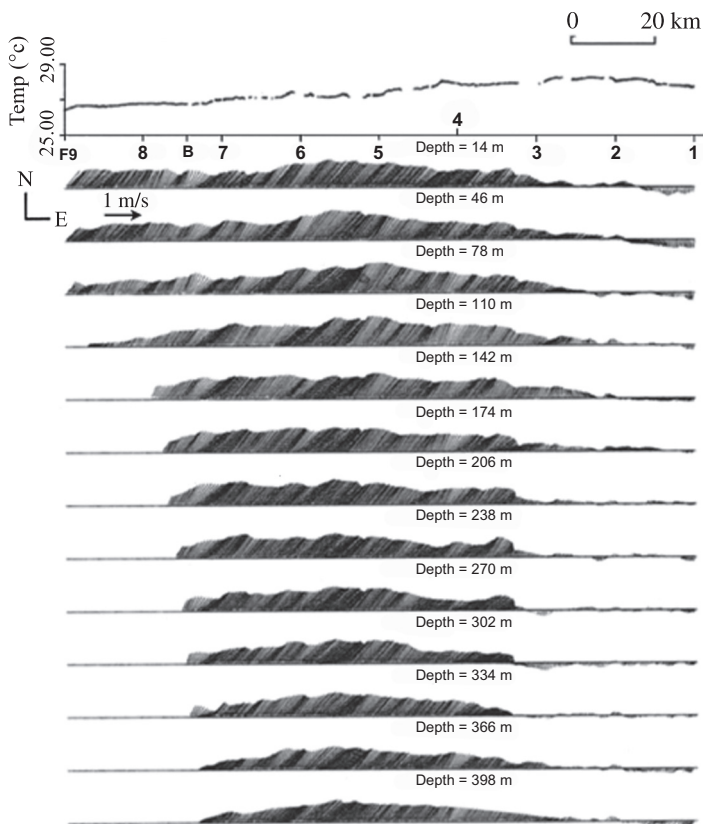


FIGURE 11.21 Vector time series (stick diagrams) of the Kuroshio horizontal current velocities obtained from towed ADCP measurement at 13 different depths. The depth scale for each diagram is inscribed just above the corresponding one. The horizontal variations of the water temperature at depth 8 m is presented at the top of the figure. (Source: Kaneko et al., 1990.)

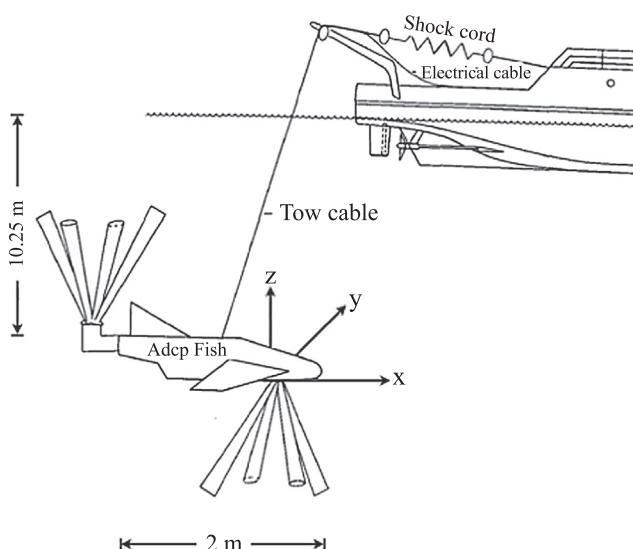


FIGURE 11.22 Sketch of towed fish consisting of a hydrodynamic body, a conducting tow cable, and two independent upward- and downward-facing ADCP systems. (Source: Monchow et al., 1995, ©American Meteorological Society, reprinted with permission.)

tow cable with 22 inner steel wires and 42 outer steel wires with an added zipper tubing cable fairing to minimize strumming, and two independent ADP systems manufactured by RD Instruments. The cable is rolled onto one of the winches aboard the towing vessel and paid over the stern or the side through a 0.52-m-diameter block on the aft A-frame or side crane. A shock-cord assembly, consisting of 10 strands of 0.02-m-wide and 3-m-long bungee cord, is fastened to the cable using Yale Minigrip Kevlar braid grips. The shock cord takes the load of the tow between the winch and the block in order to reduce peak loads on the cable due to the differential motion between the towed body and the heaving ship.

The ADPs are mounted inside an Edo Western, Inc., model 1019 hydrodynamic body. The body is about 1.5 m long and has a wing span of 1.5 m. The instrument's cavity is 0.5 m deep and 0.8 m wide and includes a 400-kg lead weight in the front side. The ADP electronics pressure cases are placed horizontally inside the cavity of the tow body. The transducer heads are coupled to the case through 90° adapters so that the 153- and 614-kHz transducers are oriented downward and upward, respectively. The pitch and roll angles are measured using tilt sensors fixed to the ADP, whereas the heading angle is

measured with two KVH fluxgate compasses, one ungimbaled and the other gimbaled. The ungimbaled compass is part of the ADP; the gimbaled one is not. A pressure sensor indicates the vertical displacements of the platform. Sampling frequencies for all these instruments are higher than 0.5 Hz, high enough to resolve motions that are induced by surface gravity waves.

This towed ADP system was deployed from ships of opportunity and towed at depths between 5 and 25 m. The instrument platform (fish) was found to be stable in most operating conditions at ship speeds up to 4.5 m/s. [Munchow et al. \(1995\)](#) identified two separate sources of errors in their tow system: surface gravity waves and compass biases. Surface gravity waves add noise into the compass record dominantly through the rolling motion of the platform. Other variables such as pitch and vertical displacement appear to be unimportant. Under most operating conditions, however, variations in pitch, roll, and vertical position do not exceed 0.5°, 0.4°, and 20 cm, respectively. These variations are random and can thus be removed by averaging. Thus, the towed ADP system shown in Figure 11.22 constitutes a very stable system. Only in the presence of very choppy seas at ship speeds exceeding 3 m/s does the platform become unstable and the data it returns become unusable. Reducing the ship speed to 3 m/s alleviates the problem.

A more serious problem relates to compass biases. It was found that both the ship and the tow platform induce magnetic fields that bias the towed ADP compass. To overcome this problem, an *in situ* compass calibration scheme using GPS data ([Joyce, 1989](#)) was found to be necessary. [Munchow et al. \(1995\)](#) found errors in excess of 50 cm/s in the absence of such a calibration. Experience shows that it is important to apply the compass calibration in post-processing, prior to any averaging. Collecting single-ping data in beam coordinates is recommended, even though this increases the volume of data that needs to be stored during an experiment.

It is generally agreed that the ADP system must be towed as deeply as possible in order to minimize the effect of the ship's hull. The use of an upward-looking ADP allows deep tows while still resolving the surface layer. The ease of deployment from ships of opportunity and the capacity of the tow system to provide profile measurements from above and below the platform with different frequencies and thus different vertical resolutions are found to be of much practical value. These features enhance its flexibility and usefulness, especially to study surface and bottom boundary-layer processes.

A towed ADP system that is much different from those discussed so far and that was used to support operational monitoring of deepwater currents was reported by [Anderson and Matthews \(2005\)](#). They used a unique tow-fish system employing a 75-kHz RDI Long Ranger ADP

packaged inside of a large Endeco/YSI type 850 V-Fin. The V-Fin is approximately $1.3 \times 1.4 \times 0.7$ m and weighs 185 kg in air. This large towed body has a proven functional design, and similar systems have been used to deploy acoustic equipment for bathymetric and biological surveys. In the present case, the first beam of the ADP is aligned with the nose of the towed body. The ADP has an embedded compass to detect the system orientation, along with pressure and tilt sensors. An electromechanical tow cable provides both data and power. The tow fish is deployed at nominally 20 m depth with tow speeds of 1 to 3 m/s.

The tow cable is deployed through a sheave on the A-frame. The towed-body configuration provides a quiet and stable sensor platform that could be readily relocated and deployed from different vessels. During sea trial by [Anderson and Matthews \(2005\)](#), wind speed was in the range 4–6 m/s and significant wave height was 0.5 m. Under such meteorological and sea-state conditions, the mean (and standard deviation) of the pitch and roll of the tow-fish system were -11.0 (1.1) and -2.5 (0.6) degrees, respectively. On a later deployment, sustained wind speeds and significant wave height reached 11.0 m/s and 1.6 m, respectively. In this case, the mean (and standard deviation) of the ADP pitch and roll were -6.0 (2.9) and -1.1 (0.6) degrees, respectively. The nose was tilted slightly downward, with more motion in the pitch. The roll statistics were almost the same as under light wind conditions. Thus, the platform was found to be very stable, but the ADP system was tilted slightly with the nose down. It was observed from various deployments that the mean pitch varies with ship speed. Improved performance is expected if the V-Fin can be flown completely level.

[Anderson and Matthews \(2005\)](#) successfully deployed the V-Fin towed ADP system in the Gulf of Mexico to track the strong currents associated with the Loop Current and Loop Current eddies (LCE), which are mesoscale features in near-geostrophic balance. LCE currents usually extend to 400 m or deeper. In this operation the ship cruised at around 3 m/s. The tow fish was deployed at 20 m depth, and the first bin was centered near a depth of 44 m. The ADP provided continuous along-track profiles with good data down to the instrument's maximum range of 500 meters.

However, the range performance is linked to the pitch of the V-Fin. Raw data were telemetered to shore for processing and integration with satellite imagery and other *in situ* observations to provide a real-time synoptic analysis. The example includes strong currents from an anti-cyclonic eddy. It also shows layers of fine-scale shear that are particularly noticeable at the edge of the eddy between 35 and 65 km along the track. These layers are coherent for 5 or more kilometers and might indicate an enhancement of near-inertial internal wave active in the thermocline along the edge of the eddy. It is considered that the ADP mounted

on this towed-body system is able to resolve such fine scale variability because it is so stable.

A disadvantage with this towed-body approach is that the ADP would be deployed deeper than a hull- or side-mounted system, and as a result, a single downward-looking ADP would not be able to sample the very near surface. Placing a second ADP configured in an upward-looking direction would allow profiling to the surface. Fortunately, there is room on the V-Fin to add a small (high-frequency) upward-looking ADP, if required.

ADPs operating at 300 kHz to 1.5 MHz have been successfully used in towed bodies for some time now and have performed quite well. In general, high-frequency ADPs are used in towed bodies for shallow-water applications. According to some reports, towed ADPs are not a panacea for all the problems observed in vessel-mounted systems. For example, in a towed ADP system, Monchow et al. (1995) found two separate sources of error: surface gravity waves and compass biases. They concluded that the towed ADP system returned data of the same quality as a vessel-mounted ADP system. From the divergent experiences reported by different users, it appears that the success of towed ADP systems depends primarily on the hydrodynamic stability of the towed system (and therefore on the design of the tow system) and implementation of proper *in situ* calibration procedures.

11.9. LOWERED ADCP (L-ADCP)

Technologies available until the late 1980s for profiling currents over ranges greater than 1,000 m all suffered from several disadvantages that severely limited their use. Hence, there was a major scientific need for a new profiling method with desirable characteristics such as $\sim 5,500$ m depth range, 20-m vertical resolution, accuracy of 2 cm/s or better, requiring little or no additional ship time, and available at a reasonable cost.

As noted in the preceding sections, ADPs have conventionally been used primarily in fixed applications (in side-looking or bottom-mounted configurations, or moored CMs) or hull-mounted on ships or tow bodies, with horizontal ship/tow-body motion removed through analysis of surface navigation data.

It is believed that the first use of a self-contained ADP attached to a CTD and lowered with a standard hydrographic wire was for a study of the hydrothermal plumes in 2,200 m of water at Juan de Fuca Ridge (Thomson et al., 1989). This arrangement is known as *lowered ADCP*, nicknamed *L-ADCP*. Although the main interest of these researchers was in examining the velocity structure in the plume within a few hundred meters of the bottom, it was recognized that the velocity profiles collected while the instrument was being lowered could be patched together into a 2,000-m profile. In principle, the L-ADCP provides

full water-column absolute velocity profiles, coincident with CTD measurements. It also has the advantage of not requiring any extra ship time and being independent of auxiliary bottom-mounted hardware.

Close on the heels of the successful experiment by Thomson et al. (1989), Firing and Gordon (1990) mounted a downward-looking 300-kHz ADP on a rosette sampler with a CTD frame and collected valuable full-water-column vertical profile data of horizontal currents. In this arrangement, the L-ADCP measures the velocity of water current relative to the profiler, obtaining a vertical profile over a range of 100 m or so about twice per second. The motion of the ADP relative to the ground (fixed reference) is unknown, but the first difference of the velocity profile (the shear profile) is invariant (Firing and Gordon, 1990).

Averaging all such measurements of shear in depth bins as the package moves through the water column yields a shear profile for the whole water column. Integration of this vertical shear profile then gives a velocity profile relative to an unknown constant of integration. The constant can be determined if the absolute velocity of the ADP is measured by tracking the seafloor at the deepest part of the profile or by using accurate navigation such as GPS to fix the position of the ADP at launch and recovery times.

Firing and Gordon (1990) reported the results of theoretical evaluation and extensive field testing of the L-ADCP during 1989 via the Hawaii Ocean Time series (HOT) set of approximately monthly cruises north of Oahu and on a Line Islands Array (LIA) cruise from Hawaii southward across the equator. Prior to these cruises, Firing and Gordon carried out error simulation that indicated that the theoretical lower bound on velocity errors could be reduced to 2 cm/s or less, as desired. In these field measurements, the L-ADCP was equipped with a flux-gate compass and tilt sensors. The rosette frame was balanced so that the typical tilt was about 3° . Ensemble-averaged tilt and heading and their standard deviations were recorded with each ensemble and were found to be quite stable. The L-ADCP measured and recorded vector-averaged velocity in Earth coordinates for 10-s ensembles. The deepest cast was about 5,000 m.

Apart from some failures and a “mysterious problem” that caused intermittent loss of data (low percentage of data accepted in all depth bins in some ensembles) in the deepest four profiles, the L-ADCP worked normally at all depths. The profile measurements made by the L-ADCP clearly showed the “equatorial deep jets” that, compared with past profile measurements (Firing, 1987), led to the conclusion that these jets change their vertical positions over several years.

Since the successful experiments by Firing and Gordon (1990), the L-ADCPs have collected hundreds of profiles (Firing and Hacker, 1994). Wilson (1994) used an RD Instruments (RDI) 150-kHz broadband ADCP (BB-ADCP)

by mounting it on a CTD frame to measure current-velocity shear (i.e., rate of change of current velocity with depth) below the instrument during casts as deep as 5,500 meters. However, it was found that some practical aspects needed to be considered before using the broadband ADP. For example, initial tests with a low-power (40 Watt acoustic power/beam) 150-kHz BB-ADCP in June 1992 proved unsatisfactory, with range decreasing to nearly zero below 1,500 m depth. RDI subsequently introduced a high-power (240 W/beam) module for the 150-kHz BB-ADCP. Although this modification increased the range to around 150 m at the low scattering levels found below 2,000 m, it drained a standard alkaline battery pack in around 4 hours, which is the duration of a typical deep CTD cast.

Accordingly, the standard RDI pressure housing had to be modified to accept an external rechargeable battery pack. Thus, the enhanced electrical power consumption of the required high-power module necessitated modification of the standard instrument to utilize external rechargeable battery packs. Despite such difficulties, using GPS navigation data and the measured velocities, the profiles could be referenced to produce absolute velocity profiles for both the up and down casts after making correction for sound velocity using ADP temperature and a standard salinity of 35.0 ppt. [Wilson \(1994\)](#) found that data collection and processing methods have improved so much that accuracies comparable to those of the acoustically tracked dropsonde Pegasus ([Spain et al., 1981](#)) can be achieved.

A method proposed for referencing L-ADCP profiles is using bottom tracking to measure absolute velocities in the lower part of the profile. The broadband firmware allows “intelligent” bottom tracking so that the instrument does not waste time with bottom pings while out of range. [Fischer and Visbeck \(1993\)](#) have described advances in lowered profiling and associated data-processing techniques using deep profiles collected with a 150-kHz ADP as examples.

11.10. ADPs FOR CURRENT PROFILING AND AUV NAVIGATION

Applications of ADPs have extended beyond the domains of remote measurements of subsurface currents and sea surface waves. AUV navigation is another feather added to the cap of ADPs. These are briefly addressed in the following sections.

11.10.1. AUV-Mounted ADPs for Current Profiling

Apart from a variety of mobile platforms discussed so far for ocean-current profile measurements, *autonomous underwater vehicles* (AUVs) have also begun to be used for such measurements. By merging data acquired by the ADP

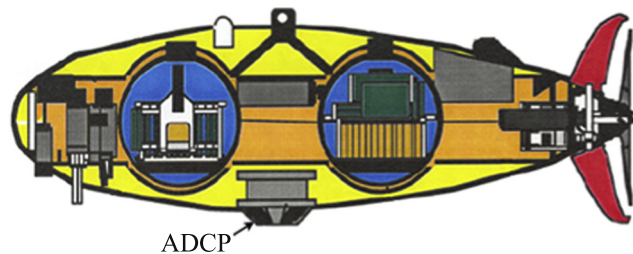


FIGURE 11.23 AUV Xanthos with downward-facing RDI ADCP in its midsection. (Courtesy of Dr. James Bellingham. Source: Y. Zhang and J. S. Willcox, *Current Velocity Mapping Using an AUV-Borne Acoustic Doppler Current Profiler*, Proc. 10th International Symposium on Unmanned Untethered Submersible Technology, pp. 31–40, Durham, NH, USA, Sept. 1997.)

with those acquired by other AUV-borne instruments as well as a long baseline (LBL) acoustic navigation system, it is possible to better observe and interpret the underwater processes of interest by utilizing AUVs. This capability was demonstrated by [Zhang and Willcox \(1997\)](#) in a field experiment at Haro Strait, British Columbia, Canada, in the summer of 1996. They developed ADP data acquisition and processing methods for AUV-mounted use.

The method Zhang and Willcox adopted in their measurements is as follows: An ADP is mounted at the midsection of an AUV in a downward-looking configuration, as shown in [Figure 11.23](#). A mission-specific ADP setting is written into the AUV mission file. Just prior to vehicle launch, a software command wakes up the ADP for pinging via an additional circuit board. The ADP is powered by the vehicle’s battery pack, and communication with the vehicle’s computer system is through an RS-232 port. The ADP is programmed to map a specific column of water (say, 100 m) during the AUV flight. This water column is subdivided into several depth bins. With measurements from its four beams, water current velocities to the specified depth relative to the flying AUV are recorded in the ADP’s internal memory and downloaded after missions onto a PC via an external RS-232 cable.

Because the ADP’s platform (the AUV) is moving, the vehicle’s velocities must be removed vectorially to obtain the current velocities relative to the Earth. If bottom track is not available, LBL navigation data may be used for estimating the vehicle’s position and horizontal velocity. For the LBL navigation using four sonar beacons, the position accuracy is better than 10 m, and the precision is better than 2 m when the vehicle’s distance from the center of the four-beacon array is less than the array aperture. The ADP clock is automatically synchronized with the vehicle clock at the beginning of each mission, thereby removing the need for data synchronization in post-processing. The vehicle’s vertical velocity is estimated from the time derivative of the depth measurements made by its depth sensor. The vehicle’s depth sensor (Paroscientific Model 8B-4000) has an

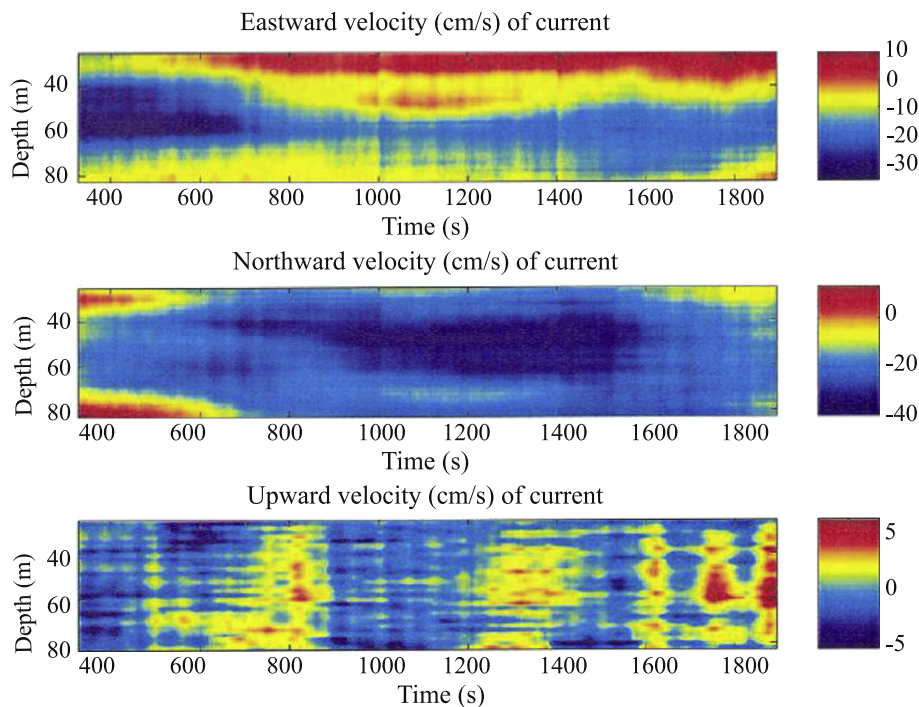


FIGURE 11.24 Earth-referenced current velocities made by an AUV (Xanthos)-mounted ADCP probe. (Source: Y. Zhang and J. S. Willcox, *Current Velocity Mapping Using an AUV-Borne Acoustic Doppler Current Profiler*, Proc. 10th International Symposium on Unmanned Untethered Submersible Technology, pp. 31–40, Durham, NH, USA, Sept. 1997.)

accuracy of 0.4 m, and its precision is better than 0.2 m. The length of the smoothing window is determined based on the measurement errors introduced by the ADP, the LBL navigation system, and the vehicle's depth sensor. The window length is adjustable to achieve a good trade-off between the temporal resolution and the estimation error relative to the maximum current velocity.

At Haro Strait, the ADP was programmed to map a 100-m column of water that was subdivided into 50 2-m depth bins. During a yo-yo mission, the AUV crossed a front, and significant contrasts of temperature and salinity between the two sides of the front were detected. Figure 11.24 shows the Earth-referenced current velocities after removing the vehicle's velocities. Processed ADP data show that the water flowed mostly southward, with the maximum southward velocity of 40 cm/s. The eastward velocity plot demonstrates a layered structure: The upper 40 meters of the water column flowed to the east at about 10 cm/s, whereas the water below flowed to the west with velocity up to 30 cm/s. This kind of layered current structure is attributed to the mixing process.

In Figure 11.25, the vertical current velocity, the vehicle's depth, and the measured temperature and salinity are compared. At time 600 s, the vehicle crossed an oceanic frontal system, entering a lower-temperature and higher-salinity water mass. Subsequently, at time 1,200 s, the vehicle turned around, and at time 1,700 s it crossed the

front again and came back to the higher-temperature and lower-salinity water mass. These signatures were well recorded by the temperature and conductivity sensors. The vertical current velocity shows that within the lower-temperature and higher-salinity region, there was downwelling of up to 5 cm/s, whereas in the higher-temperature and lower-salinity region, upwelling on the order of 5 cm/s existed. The observed alternating upwelling and downwelling events provide insight into the complexity of the mixing process. Current velocity mapping and ancillary measurements utilizing state-of-the-art technology and the AUV's role as a high-performance mobile instrumentation platform provide insight into temporal scales of the mixing process.

11.10.2. ADPs for AUV Navigation

Frequently, AUVs need to operate in ocean environments characterized by complex spatio-temporal variability. This spatio-temporal complexity is induced by the turbulent nature of the ocean, described by the continuous change of a wide range of spatial and time scales. Energetic flows induced by tides and topographic perturbations, as well as instabilities and currents induced by local wind effects, are only a few examples of ocean variability. Such variability can strongly perturb safety conditions and development of AUV operations. In particular, AUVs usually encounter

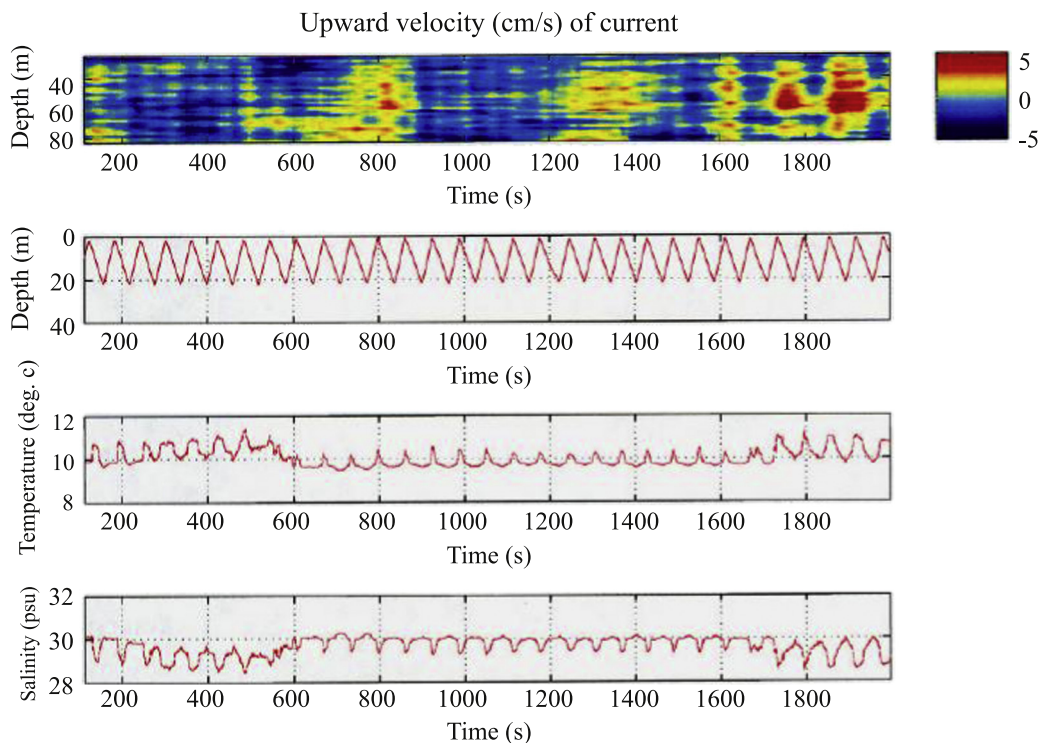


FIGURE 11.25 Earth-referenced vertical current velocity and CTD measurements made by an AUV (Xanthos)-mounted ADCP and CTD probes. (Source: Y. Zhang and J. S. Willcox, *Current Velocity Mapping Using an AUV-Borne Acoustic Doppler Current Profiler*, Proc. 10th International Symposium on Unmanned Untethered Submersible Technology, pp. 31–40, Durham, NH, USA, Sept. 1997.)

strong current fields in the marine environment that can jeopardize their missions. Robustness of AUVs to this strong environmental variability is a key element to carry out safety and optimum operations.

Determining and predicting ocean currents is a fundamental requirement to increase AUV robustness to ocean variability. *A priori* knowledge of this ocean variability would allow us to adequately plan AUV missions, thereby minimizing the possible negative effects of the environment on its operation. Unfortunately, present oceanographic technology is only capable of forecasting the large and slow components of ocean variability, since there are fast and small scales of variability that are still unpredictable. This partial knowledge about future environmental conditions degrades AUV robustness, thereby reducing its autonomy and safety. To circumvent this problem, Garau et al. (2006) proposed a class of real-time algorithm to support AUV navigation in strong, turbulent ocean environments characterized by unpredictable small-scale variability. The algorithm infers the two-dimensional structure of the current field in a limited region in front of the AUV, using the one-dimensional current flow information obtained from a horizontal ADCP known as *H-ADCP*. Subsequently, a planner locally optimizes the performance of the AUV in the inferred field by reducing the traveling time. Based on simulated turbulent environments, it was

found that the solutions provided by the algorithm required significantly less traveling time than straight-line paths.

To obtain the required one-dimensional current-flow information in a limited region in front of the AUV for optimizing its performance, a long-range H-ADCP is incorporated in the AUV's payload. The H-ADCP acoustically measures the current flow velocity profiles in a horizontal line up to ~ 300 meters in front of the AUV in more than 100 horizontal cells. Apart from the possible use of the water-current velocity profiles gathered from the H-ADCP for a variety of applications, the profiles are primarily employed by the AUV to infer the local spatial pattern of the current field to introduce the required course correction to locally optimize the AUV's navigation and safety in the region by avoiding areas with strong and complex current fields that could jeopardize the AUV mission.

In a first step, the algorithm infers from the H-ADCP profile the current field pattern in an area in front of the AUV. The inferred current field is obtained by considering that the turbulent field results from the superposition of a distribution of vortices known as *viscous Lamb vortices* (Lamb, 1932). The number, centers, and intensities of the vortices closest to the AUV are determined from the H-ADCP profile. Superposition of the current fields generated by the different vortices provides an estimation

of the spatial current distribution. Subsequently, based on the reconstructions from the H-ADCP profile and a searching procedure for finding the local minimum-time paths, the AUV plans the trajectory with minimum traveling time in the reconstructed region, trying to take full advantage of the current field that locally favors its mission and to support the AUV navigation to find the way to reach the goal destination, avoiding the hazardous high-speed currents around the goal area. The procedure is repeated when the AUV reaches the border of the inferred current field or when a need to update the inferred current field is detected.

11.11. CALIBRATION OF ADPs

Experiments under controlled conditions are needed to establish the absolute performance of a measuring instrument. In the case of an ADP, calibration in a tow-tank facility enables estimation of its performance. However, unlike conventional Eulerian-style CMs, ADPs have some limitations for being calibrated in a tow tank. These limitations arise primarily from the relatively small size of the tow tank in terms of its width and depth. First, the beams of an ADP are divergent, because of which they intersect with the side walls of the tow tank beyond a certain slant range. Second, the bin length needs to be sufficiently small in size so that the bin is comfortably confined well within the tow tank. Third, the measurements tend to be contaminated by side-lobe interference from the bottom/water surface of the tow tank.

The first limitation is insurmountable, given the large depth range of most of the ADPs. However, the second problem can be resolved by the use of high-frequency ADPs (in effect, shallow-water ADPs) so that pulse length τ is considerably small. In the case of the third limitation, solutions have been found to take care of the problems arising from side-lobe interference. It has been theorized that the acoustic side-lobe energy could be deflected and/or absorbed. The idea embodied in this theory is to develop a device that would allow the main beam to progress undisturbed but restrict the propagation of the side lobes.

NOAA has conducted experiments during field tests with prototype baffles, yielding encouraging results (Appell, 1984; Appell et al., 1985). These tests were conducted in the early 1980s with an AMETEK Straza 300-kHz system. The device consisted of a cone-shaped baffle that was placed between the beams. Side lobes would strike the baffle and be reflected in a horizontal direction. Stray acoustic energy coming from the surface would be reflected and/or absorbed by the top surface of the baffle.

In subsequent tow-tank studies, Appell et al. (1991) subjected RD 1200-kHz and 600-kHz ADPs to tow-tank tests in the David Taylor Research Center (DTRC) towing basin to investigate ADP accuracies. In these

experiments, the ADPs could be calibrated in the first four bins (bin 5 indicated signs of contamination) in a downward-looking mode. The ADP parameters were set during DTRC tests (in upward-looking configuration) to provide 1-m bin lengths. During those tests it had been observed that side-lobe returns from the concrete basin bottom biased the measurements at 85 percent (bin 5) of the range. It was also noted that the next bin (bin 6) was not contaminated. In the DTRC tow-tank tests, a 1,200-kHz ADP with a right-angle head adapter was mounted on a bottom sled in an upward-looking mode. The sled was guided by a drainage trough that ran the length of the basin. The sled-borne ADP was towed from the carriage using two tow lines for stability. One end of the tow basin contained a pneumatic wave maker. Maximum amplitude waves of 1-m peak-to-peak were achievable at a 3-s period. An acoustic wave gauge was mounted on the carriage to acquire wave height measurements simultaneously with ADP current measurements.

The bin length (governed by pulse length τ) was set to 1 m and blanking distance to 0.5 m. The tests were conducted with beams 3 and 4 aligned in the towing direction and beams 1 and 2 cross-channel. Data were recorded in beam coordinates so that performance of each beam in the preferential orientation of the ADP could be evaluated on an individual basis. Simultaneous inputs from the tow carriage-speed measurement system and wave gauge were recorded.

Tests were conducted under a variety of tow-speed and surface-wave conditions. A cone-shaped baffle attached to the ADP head prevented side-lobe contamination of the ADP measurements. Tow-tank test results yielded the basic features of the ADP. For instance, zero-flow conditions showed a positive 1 to 2 cm/s bias in all beams and bins. Tow speeds of up to 100 cm/s contained beam errors of within ± 2 cm/s in the first three bins. Bin 1 had occasionally higher errors of up to 4 cm/s. Bin 4 (estimated to be at 85 percent of the range and therefore expected to receive the side-lobe energy) consistently had negative errors of 4 to 10 cm/s in the absence of baffle. However, the results in bin 4 were dependent on the size of the baffle. For instance, small baffle did improve the performance of bin 4. However, the larger size baffle showed marked improvement.

These results indicate that the baffle must block sufficient side-lobe energy to be effective. The small baffle did not provide sufficient blockage. With the larger baffle, errors in bin 4 were reduced to normal system errors, showing no signs of the negative bias. Bin 1 showed a slight negative bias compared to the no-baffle data, the reason for which remains to be unknown. With the incorporation of the baffle, bin 5 returned to a normal range of errors.

The tow-tank tests under different artificially generated surface-wave conditions revealed that the frequency content of the wave spectra was produced accurately in the

profiler data. Tow-tank wall reflections of wave energy produced velocities in the cross-channel beams. However, wave-particle velocities in the water column had no adverse effect on the ability to determine the “mean” flow.

In a nutshell, based on tow-tank test results of Appell et al. (1991), the 1,200-kHz ADP demonstrated the ability to accurately measure mean currents in a wave-laden flow field. It has been found that side lobes can bias the measurements at 85 percent of the range when bottom or surface boundaries are present. The amount of bias is strongly dependent on surface wave characteristics. Side-lobe bias can be eliminated with a properly designed baffle system. Appell et al. (1991) also demonstrated the ADP’s ability to measure water wave particle velocities with a properly configured system (e.g., high transmission frequency and fine sampling interval).

Tow carriages employed for the purpose of calibration of water-flow measuring devices are of various constructions. The drainage trough as available in the DTRC tow basin is not a common feature of every tow basin. Furthermore, the mounting arrangement for the ADP under calibration needs to have the facility to be tilted and rotated so that the acoustic beams can be properly oriented in any desired direction to accomplish different test conditions.

Joseph et al. (2003) reported the design and successful application of a mounting device for a Doppler Velocity Log (see Figure 11.26), which permitted its tilting at roll angles, pitch angles, and combinations of a multitude of chosen roll and pitch angles. Choice of minimum possible projected areas for the components used in the mounting device substantially reduces motion-induced drag force during towing. The edges of all the components of the mounting mechanism are rounded or chamfered to reduce

flow separation and shedding. The mechanism is easy to assemble and mount and is amenable to quick changes of angles. A protractor, mounted on a plane, which is perpendicular to the axis of the support rod, is used for measurement of the horizontal azimuthal directions of the device under calibration. The mounting device was successfully used to examine the performances of a 500-kHz, three-beam downward-looking Sontek Argonaut acoustic Doppler velocity log (DVL).

Figure 11.27 shows a tow tank and towing facility at Central Water & Power Research Station (CW&PRS) at Pune, India, together with the DVL and its mounting attachment. This mounting arrangement can be conveniently used for calibration and performance evaluation tests of an ADP in downward-looking, side-looking, or inclined directions.

11.12. INTERCOMPARISON AND EVALUATION

As in the case of other types of CMs, several aspects of acoustic profiler system performance can, in principle, be evaluated by applying several different techniques. Most of the performance evaluation studies have involved comparison with independent forms of measurement. However, an important step forward has been the development of system-modeling techniques (Chereskin et al., 1989; Chereskin and Harding, 1993). As noted by Chereskin and Harding (1993), this approach, applied in conjunction with signal simulation, enables the performance of individual parts of the system to be analyzed and allows the relationship between system parameter choice and measurement error to be investigated.

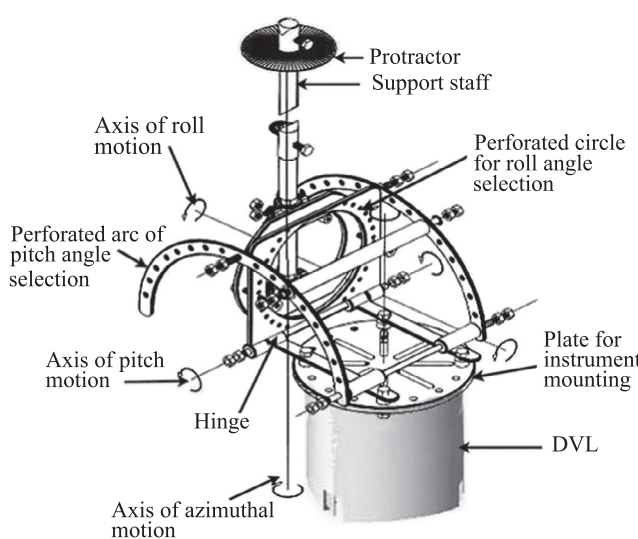


FIGURE 11.26 Support-mechanism for tow-tank experiments on an Acoustic Doppler Velocity Log. (Source: In part from Joseph et al., 2003.)

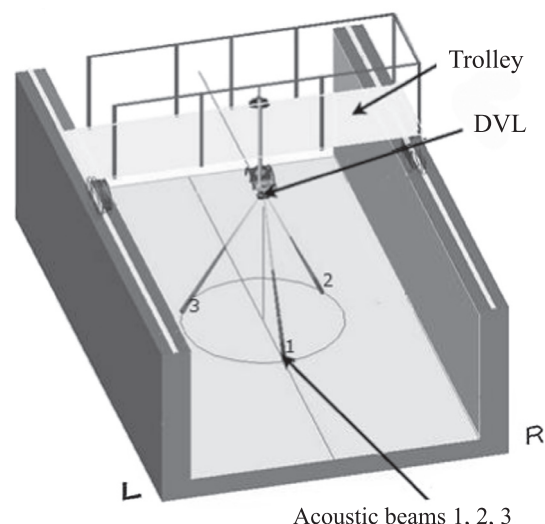


FIGURE 11.27 Tow tank and towing facility, together with the DVL and its mounting attachment. (Source: Joseph, A., CSIR, National Institute of Oceanography, Goa, India.)

A number of intercomparison studies have been carried out on ADPs by several researchers, and most of them have been associated with upward-directed ADPs deployed on the seabed in shelf seas, particularly in coastal areas, although Schott (1986), Schott and Johns (1987), and Johns (1988) investigated the use of profilers in deep water for the purpose of obtaining long time series of currents.

For the most part, intercomparisons have been made using data from moored CMs of various types, although Griffiths (1986) has also compared current profiles derived from a Doppler sonar with the predictions of a shallow-water tidal model and found an excellent measure of agreement (Collar, 1993). Figure 11.28 shows current amplitude profiles measured at 3 hours after high water over a number of successive tidal cycles. These have been normalized to water depth D and depth-mean current \bar{U} and clearly show the classical form associated with a logarithmic bottom boundary layer, for which:

$$u(z) = \frac{u^*}{k_o} \ln(z/z_o) \quad (11.17)$$

where:

k_o = von Karman's constant ($= 0.4$ in clear water)

z_o = a roughness length constant

z = height above bottom

u^* = shear velocity

Close agreement is evident among the measured profile, the output from an analytical tidal model, and independent bottom observations. The slight offset between the ADP output and the model has been attributed to inaccuracy in extracting a true depth-mean current from the ADP data.

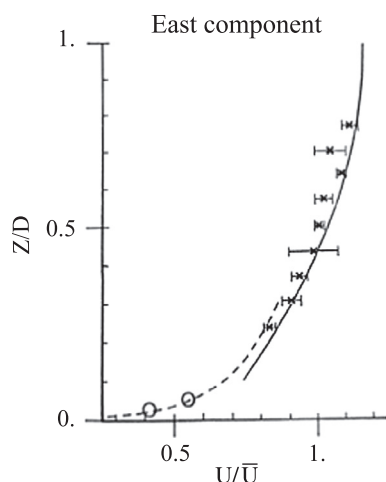


FIGURE 11.28 Normalized profiles of water-current amplitude obtained from a bottom-mounted ADP in shallow water. (*) ADCP with 95-percent confidence limits; (—) analytical model; (----) theoretical bottom boundary layer; (\bar{U}) depth-mean current. (Source: Collar, 1993, reproduced with kind permission from Jane Stephenson, National Oceanography Centre, Southampton SO14 3ZH, UK.)

The published results of other instrumental comparisons broadly suggest that below the surface wave zone, incoherent acoustic Doppler provides comparable accuracy of measurement to that of vector-averaging discrete instruments, although Magnell and Signorini (1986) found some discrepancies between data from an ADP and moored instruments at periods outside the main tidal bands. In another study, Pettigrew et al. (1986) found generally excellent agreement between a bottom-mounted ADP and moored VACM and VMCM data. In these studies, the differences observed within 20 m of the surface were consistent with motion-induced errors previously identified in laboratory studies on VACM and VMCM instruments. A subsequent study (Freitag et al., 1992) showed that in some circumstances, ADP speeds can be biased low in comparison with speeds recorded by moored instruments. This is attributed to the presence of fish school in the ADP beams.

Cochin et al. (2006) reported intercomparison studies between an ADP and pulsed VHF Doppler radar systems (VHF COSMER system) in Normand Breton Gulf, France, where the tidal elevation range is about 11 m and the maximum water current velocity is around 2 m/s. During the experiment, the ADP measurements were collected at 10-min intervals. The ADP was configured to make measurements at 28 bins, each with a length of 1 m. Each measurement represented current that was integrated over two bins (i.e., 2 m). On peak spring tide, the sea surface was located above the upper bin (more than 30-m depth).

For intercomparison studies, measurements from a fixed immersion were extracted, taking into account the blind zone of the instrument, which was 4 m below the sea surface. Evaluation of subsurface ADP current measurements was carried out against surface currents obtained from the VHF COSMER pulse-Doppler radar system (the precision of which is around 2 cm/s) and simulation from hydrodynamical numerical model TELEMAC 2-D, developed by the Laboratoire National d'Hydraulique et Environnement (EDF-LNHE), France. Numerical model simulations represent estimation of surface currents, with a mean error of 10 percent. For a fair comparison between the ADP and radar measurements, tidal currents have been extracted from both measurements by subtracting the mean residual current (which is primarily due to meteorological influences) from the observed datasets. Time series of the vector currents (U is the east component and V is the north component) showed that the maximum sea surface currents measured by the instruments yielded different speeds and directions. The observed differences are mainly due to the different techniques of acquisition (Graber et al., 1997).

For example, the electromagnetic method (VHF COSMER) yields a spatially and temporally averaged

surface current measurement and is limited to observation near the sea surface, whereas the acoustic method (ADP) produces a subsurface point measurement into bins of the water column. Furthermore, higher time integration and temporal resolution might smooth the currents (which can change rapidly, particularly in spring tides). The observed differences can also be explained by geophysical variability, especially close to the coast (ADP position), where currents are spatially variable (horizontal and vertical).

The presence of an island in the area (east of Pointe du Grouin) creates a channel with strong currents during ebb, oriented toward the ADP position. Those currents are measured by the ADP (one measurement every 10 min), whereas the radar measurements smooth them (spatially over approximately 1 km² and temporally over 9 min, with one measurement every 30 min). This comparison clearly reveals the complementarities of two different technologies.

Based on examination of numerous intercomparison studies carried out in the initial decades of ADP measurements, Collar (1993) concludes that if adequate leveling of the instrument can be arranged, the use of bottom-mounted ADPs provides substantial advantages over strings of moored CMs in determining vertical profiles of currents. The reasons include the following (Collar, 1993):

- The flow is completely unobstructed by the sensor.
- Measurements are not contaminated by instrument motion.
- Any compass-related errors are common at all levels (bins).
- Relative errors arising from this cause should be small.
- The instrument is probably more secure than a moored string of CMs.
- Costs, including maintenance, are lower than those relating to an equivalent series of discrete instruments.

Instrument tilt can give rise to measurement errors. However, this problem can be taken care of by incorporating tilt sensors in the ADP and by accounting tilt measurements in the velocity calculations. Errors resulting from instrument tilt have been considered by Pulkkinen (1993).

The main problems arise in making measurements close to and within the surface wave zone, in which fluid motions are sheared and are highly variable in magnitude and direction. The instantaneous surface provides a strong acoustic target, as do the air bubbles carried down by the breaking waves (Thorpe, 1986). Backscattered returns may in consequence suffer spectral broadening or distortion, and if the transducer has a near-vertically directed side lobe, which is inadequately suppressed, signals at longer ranges may be masked by strong, unwanted surface returns. Errors may also be generated in determining Doppler shift in high-shear flows (Pullen et al., 1992). In

the initial years of ADP deployments and performance evaluation studies, relatively little effort seems to have been devoted to their near-surface applications, although some preliminary work has been done at the Institute of Oceanographic Sciences (IOS) in the United Kingdom using an upward-looking ADP moored at about 20-m depth (Collar, 1993). Several downward-looking, buoy-mounted systems began to be developed in subsequent years.

Shipboard ADPs have also been subjected to performance evaluation studies. Such studies have included both error analyses and comparative observations made with profiling CMs and moored instruments in both shallow and deep waters (Collar, 1993). These studies (e.g., Chereskin et al., 1987; Magnell and Signorini, 1986; Didden, 1987; Pettigrew et al., 1986; Schott, 1986; Appell et al., 1985; Griffiths, 1986; Delcroix et al., 1992) have generally shown good agreement between the respective techniques, though data on performance under severe sea-state conditions could be limited.

Apart from the physical characteristics of the acoustic medium discussed earlier, factors that have been considered in assessing the accuracy attainable in current shear measurement using shipboard ADP can include various components of ship motion, imperfections in the acoustic geometry (beam pattern, beam orientation), and acoustic noise generated by the ship itself (Joyce et al., 1982; Crocker, 1983; Didden, 1987; Kosro, 1985; Kosro et al., 1986; Joyce, 1989). Velocity quality screening techniques are an important aspect in obtaining maximum accuracy from shipboard ADPs. Real-time methods have been discussed by Zedel and Church (1987). In measurement of absolute current, the rate of change of ship position with time over the Earth's surface must be known to a higher precision than that required of the current measurement. This requirement represents a major constraint (Trump, 1986), although with full implementation of improved satellite-based position-fixing systems such as GPS, the level of attainable accuracy should show marked improvement.

11.13. MERITS AND LIMITATIONS OF ADPs

Probably the most important characteristic of the ADP is its ability to provide a substantial increase in the vertical density of current data obtainable from a single instrument. Furthermore, because the majority of measurements are made remotely, only a small part of the current field—immediately surrounding the instrument—is perturbed. Current measurements are therefore made in a theoretically ideal way. An added advantage, which is not obtainable with older-generation current profilers, is that the

acoustic system can also create profiles of acoustic back-scattering strength (Peynaud and Pijanowski., 1979). This information provides an additional window into the environment by which researchers can synoptically study the vertical distribution of biological scatterers such as plankton. The backscattered signal can also be useful to fisheries scientists, assisting them in estimating fish population. The different time responses by water layers at different depths to a fluctuating wind regime induces high lateral shear (Blanton et al., 1974). Oceanic water-current velocity shear has great importance in turbulent mixing and dispersal effects. An interesting application of ADP in oceanography is in the study of fine structures and velocity shear in the water column.

Fast profiling such as that available from an ADP is not possible with free-fall probes. Further, the ADP can map the horizontal (restricted to its field of view) as well as vertical distribution of the current field and its temporal variations. In fact, field experiments using such a profiler could yield three-dimensional current distribution patterns (Okuno et al., 1983). Results of inter-comparison experiments showed striking agreement between results from conventional Eulerian CMs and a bottom-mounted acoustic Doppler current profiler (Pettigrew et al., 1983). Current profiling over vertical ranges of hundreds of meters in the deep ocean has been achieved by an acoustic profiler mounted on top of a subsurface mooring (Schott, 1986). Special precautions must be taken, however, to obtain reliable data from near the sea surface.

Unlike the freely sinking current profiler probe addressed in the previous section, the ADPs can be made to “look” in any direction, and their deployments may be on fixed or moving platforms or on surface, bottom, or mid-depth moorings (Christensen, 1983). Furthermore, the acoustic Doppler technique permits continuous, unattended, fast profiling of currents. Remote sensing with Doppler sonar, therefore, provides an attractive alternative to all previous methods of current profile measurements. Furthermore, in situations where only short-term current measurements are needed, the capability of hull-mountable, downward-looking remote profilers to make measurements from moving vessels is a remarkable feature that permits large spatial coverage and virtually eliminates the tedious and time-consuming logistics in the deployment and retrieval, if conventional moorings were to be used. Mounted beneath a moving vessel, an ADP can make current profile measurements without the motion of the ship significantly affecting the current measurements, because the profiler can measure the speed of the ship with respect to the bottom if the survey area is sufficiently shallow that the ADP’s depth range is larger than the local depth of the seafloor beneath the vessel.

REFERENCES

- Anderson, S.P., Mathews, P., 2005. A towed 75 kHz ADCP for Operational Deepwater Current Surveys. In: Proc. IEEE/OES Eighth Working Conference on Current Measurement Technology. IEEE, New York, NY, USA, pp. 46–49.
- Andreucci, F., Camporeale, C., Fogliuzzi, F., 1992. Acoustic wideband techniques for the remote estimation of the sea current velocity. In: Proc. IEEE Conference Oceans '92. IEEE, New York, NY, USA, pp. 614–619.
- Appell, G.F., Gast, J.A., Williams, R.G., Bass, P.D., 1988. Calibration of acoustic Doppler current profilers. Proc. Oceans '88.
- Appell, G.F., Bass, P.D., Metcalf, M.A., 1991. Acoustic Doppler Current Profiler performance in near surface and bottom boundaries. IEEE J. Ocean Eng. 16 (4), 390–396.
- Appell, G.F., Mero, T.N., Sprenke, J.J., Schmidt, D.R., 1985. An inter-comparison of two acoustic Doppler current profilers. In: Proc. IEEE Conference on Ocean Engineering and the Environment, November 1985, San Diego. IEEE, New York, NY, USA, pp. 723–730.
- Appell, G.F., Mero, T.N., Sprenke, J.J., Schmidt, D.R., 1985. An inter-comparison of two acoustic Doppler current profilers. Proc. Oceans '85.
- Blanton, J.O., Murthy, C.R., 1974. Observations of lateral shear in the near-shore zone of a great lake. Journal of Physical Oceanography 4, 660–663.
- Bourgerie, R.W., Garner, T.L., Shih, H.H., 2002. Coastal current measurements using an ADCP in a streamlined sub-surface mooring buoy. IEEE 2002, 736–741.
- Brumley, B.H., Cabrera, R.G., Deines, K.L., Terray, E.A., 1991. Performance of a broad-band Acoustic Doppler Current Profiler. IEEE J. Oceanic Eng. OE-16, 402–407.
- Capon, J., 1969. High-resolution frequency-wavenumber spectrum analysis. Proc. IEEE 57, 1408–1418. also Corrigendum in Proc. IEEE (Lett.), 59, 112 (1971).
- Chereskin, T.K., Harding, A.J., 1993. Modelling the performance of an acoustic Doppler current profiler. J. Atmos. Oceanic Technol. 10, 41–63.
- Chereskin, T.K., Harding, J., 1993. Modeling the performance of an acoustic Doppler current profiler. J. Atmos. Oceanic Technol. 10, 42–63.
- Chereskin, T.K., Halpern, D., Regier, L.A., 1987. Comparison of shipboard acoustic Doppler current profiler and moored current measurements in the equatorial Pacific. J. Atmos. Oceanic Technol. 4, 742–747.
- Chereskin, T.K., Firing, E., Gast, J.A., 1989. Identifying and screening filter skew and noise bias in ADCP current profiler measurements. J. Atmos. Oceanic Technol. 6, 1040–1054.
- Chereskin, T.K., Firing, E., Gast, J.A., 1989. Identifying and screening filter skew and noise bias in acoustic Doppler current profiler measurements. J. Atmos. Oceanic Technol. 6, 1040–1054.
- Christensen, J.L., 1983. A new acoustic Doppler current profiler. Sea Technology, Feb. issue, 10–13.
- Cochin, V., Mariette, V., Broche, P., Garello, R., 2006. Tidal current measurements using VHF radar and ADCP in the Normand Breton Gulf: Comparison of observations and numerical model. IEEE J. Ocean. Eng. 31 (4), 885–893.
- Collar, P.G., 1993. A review of observational techniques and instruments for current measurements from the open sea. Report No. 304, Institute of Oceanographic Sciences, Deacon Laboratory, UK.

- Crocker, T.R., 1983. Near-surface Doppler sonar measurements in the Indian Ocean. *Deep-Sea Res.* 30, 449–467.
- Cutchin, D., Christensen, J., Knoop, R., Stillman, J., Woodward, W., 1986. Acoustic Doppler current profiling from a volunteer commercial ship. In: Appell, G.F., Woodward, W.E. (Eds.), *Proc. IEEE Third Working Conference on Current Measurement*. IEEE, New York, NY, USA, pp. 98–105. January 22–24, 1986, Airlie, VA.
- de Schipper, M.A., de Zeeuw, R.C., de Vries, S., Stive, M.J.F., Terwindt, J., 2010. Horizontal ADCP measurements of waves and currents in the very near-shore. *Proc. IEEE/OES/CWMT Tenth Working Conference on Current Measurement Technology*, 159–166.
- Delcroix, T., Masia, F., Eldin, G., 1992. Comparison of Profiling Current Meter and Shipboard ADCP measurements in the Western Equatorial Pacific. *J. Atmos. Oceanic Technol.* 9, 867–871.
- Didden, N., 1987. Performance evaluation of a shipboard 115 kHz acoustic Doppler current profiler. *Cont. Shelf Res.* 7, 1231–1243.
- Earwaker, K., Zervas, C., 1999. Assessment of the National Ocean Service's Tidal Current Program. NOAA Technical Report NOS CO-OPS 022. Center for Operational Oceanographic Products and Services, NOS, NOAA, Silver Spring, MD, USA, pp. 70.
- Firing, E., 1987. Deep zonal currents in the central equatorial Pacific. *J. Marine Res.* 45, 791–812.
- Firing, E., Gordon, L., 1990. Deep ocean acoustic Doppler current profiling. *Proc. IEEE Fourth Working Conf. on Current Measurements*. Clinton, MD, Current Measurement Technology Committee of the Oceanic Engineering Society, August 1990, pp. 192–201.
- Firing, E., Hacker, P., 1994. Equatorial subthermocline currents across the Pacific. *EOS Trans., American Geophys. Union*, 75(3).
- Freitag, H.P., McPhaden, M.J., Pullen, P.E., 1992. Fish-induced bias in acoustic Doppler current profiler data. In: *Proc. IEEE Conference, Oceans '92*. IEEE, New York, NY, USA, pp. 712–717.
- Froysa, K.G., Almroth, E., Andersson, S., Apler, A., Tengberg, A., Hall, P., 2007. Environmental monitoring: Two field cases. *Ocean Systems* 11 (2), 9–11.
- Garaa, B., Alvarez, A., Oliver, G., 2006. AUV navigation through turbulent ocean environments supported by onboard H-ADCP. *Proc. 2006 IEEE Int. Natl. Conf. Robotics and Automation*, Orlando, FL, USA. May 2006, 3556–3561.
- Gawarkiewicz, G., Wang, J., Caruso, M., Ramp, S.R., Brink, K.H., Bahr, F., 2004. Shelf-break circulation and thermohaline structure in the northern South China Sea – Contrasting spring conditions in 2000 and 2001. *IEEE J. Oceanic Eng.* 29 (4), 1131–1143.
- Gordon, R.L., 1990. A review of interesting results obtained with acoustic Doppler current profilers. In: Appell, G.F., Curtin, T.B. (Eds.), *Proc. IEEE Fourth Working Conference on Current Measurement*. IEEE, New York, NY, USA, pp. 181–191. April 3–5, 1990, Maryland.
- Gordon, R.L., Brumley, B., Terray, E.A., 1998. Observing wave height and direction with conventional (Janus-style) ADCPs. *Oceanology International '98* 2, 261–269.
- Graber, H.C., Haus, B.K., Chapman, R.D., Shay, L.K., 1997. HF radar comparisons with moored estimates of current speed and direction: Expected differences and implications. *J. Geophys. Res.* 102 (C8), 18,749–18,766.
- Griffiths, G., 1986. Intercomparison of an acoustic Doppler current profiler with conventional instruments and a tidal flow model. In: Appell, G.F., Woodward, W.E. (Eds.), *Proc. IEEE Third Working Conference on Current Measurement*. IEEE, New York, NY, USA, pp. 169–176. January 22–24, 1986, Airlie, VA.
- Hamilton, J.M., 1989. The validation and practical applications of a subsurface mooring model. *Canadian Technical Report on Hydrography and Ocean Sciences* 119. Ottawa, Ontario, Canada, pp. 49.
- Hamilton, J.M., Fowler, G.A., Belliveau, D.J., 1997. Mooring vibration as a source of current meter error and its correction. *J. Atmos. Oceanic Technol.* 14 (3), 644–655.
- Hansen, D.S., 1985. Asymptotic performance of a pulse to pulse incoherent Doppler sonar in an oceanic environment. *IEEE J. Oceanic Eng.* OE-10, 144–158.
- Herbers, T.H.C., Lowe, R.L., Guza, R.T., 1991. Field verification of acoustic Doppler surface gravity wave measurements. *J. Geophys. Res.* 96 (9), 17,023–17,035.
- Howarth, M.J., 1999. Wave measurements with an ADCP. *IEEE 1999*. New York, NY, USA, pp. 41–44.
- Johns, W.E., 1988. Near-surface current measurements in the Gulf Stream using an Upward Looking Acoustic Doppler Current Profiler. *J. Atmos. Oceanic Technol.* 5, 602–613.
- Johnson, D.H., Dudgeon, D.E., 1993. Array signal processing. Prentice Hall, Upper Saddle River, New Jersey, United States, pp. 533.
- Joseph, A., 2000. Applications of Doppler effect in navigation and oceanography. *Encyclopedia of Microcomputers*. Marcel Dekker Inc 25, 17–45.
- Joseph, A., Madhan, R., Mascarenhas, A., Desai, R.G.P., Kumar, V., Dias, M., Tengali, S., Methar, A., 2003. Evaluation of performance of SonTek Argonaut acoustic Doppler velocity log in tow tank and sea, *Proc. of the National Symposium on Ocean Electronics: SYMPOL '2003*. Department of Electronics, Cochin University of Science and Technology, Cochin, 3–12.
- Joyce, T.M., 1989. On *in situ* "calibration" of shipboard ADCPs. *J. Atmos. Oceanic Technol.* 6, 169–172.
- Joyce, T.M., Bitterman, D.S., Prada, K.E., 1982. Shipboard acoustic profiling of upper ocean currents. *Deep-Sea Res.* 29 (7A), 903–913.
- Joyce, T.M., Bitterman Jr., D.S., Prada, K.E., 1982. Shipboard acoustic profiling of upper ocean currents. *Deep-Sea Res.* 29, 903–913.
- Kaneko, A., Koterayama, W., 1988. ADCP measurements from a towed fish. *EOS* 69 (23), 643–644.
- Kaneko, A., Gohda, N., Koterayama, W., Nakamura, M., Mizuno, S., Furukawa, H., 1993. Towed ADCP fish with depth and roll controllable wings and its application to the Kuroshio observation. *J. Oceanogr.* 49, 383–395.
- Kaneko, A., Koterayama, W., Honji, H., Mizuno, S., Kawatake, K., Gordon, R.L., 1990. Cross-stream survey of the upper 400 m of the Kuroshio by an ADCP on a towed fish. *Deep-Sea Res.* 37 (5), 875–889.
- King, B.A., Cooper, E.B., 1993. Comparison of ship's heading determined from an array of GPS antennas with heading from conventional gyrocompass measurements. *Deep-Sea Res.* 40, 2207–2216.
- Kirby, J.T., Chen, T.-M., 1989. Surface waves on vertically sheared flows: approximate dispersion relations. *J. Geophys. Res.* 94 (C1), 1013–1027.
- Kosro, P.M., 1985. Shipboard acoustic current profiling during the Coastal Ocean Dynamics Experiment. *Scripps Institution of Oceanography, Research Theses and Dissertations, California Sea Grant College Program*, UC San Diego, CA, USA, Ref, 85–8, pp. 119.
- Kosro, P.M., Regier, L., Davis, R.E., 1986. Accuracy of shipboard Doppler current profiling during CODE. In: Appell, G.F.,

- Woodward, W.E. (Eds.), Proc. IEEE Third Working Conference on Current Measurement. IEEE, New York, NY, USA, p. 97. January 22–24, 1986, Airlie, VA.
- Krogstad, H.E., Gordon, R.L., Miller, M.C., 1988. High resolution directional wave spectra from horizontally-mounted Acoustic Doppler Current Meters. *J. Atmos. Oceanic Technol.* 5, 340–352.
- Lamb, H., 1932. Hydrodynamics. Cambridge University Press, 738.
- Lhermitte, R.M., 1985. Water velocity and turbulence measurements by pulse coherent Doppler sonar. In: Proc. IEEE Conference Oceans '85: Ocean Engineering and the Environment. IEEE, New York, NY, USA, pp. 1159–1164. November 1985, San Diego.
- Lhermitte, R.M., Serafin, R., 1984. Pulse-to-pulse coherent Doppler sonar signal techniques. *J. Atmos. Oceanic Technol.* 1, 293–230.
- Lohrmann, A., Siegel, E., 2010. Waves in the summer ice in the winter. In: Proc. IEEE/OES/CWTM Tenth Working Conference on Current Measurement Technology, pp. 150–158.
- Lohrmann, A., Hackett, B., Roed, L.P., 1990. High resolution measurement of turbulence, velocity and stress using a pulse to pulse coherent sonar. *J. Atmos. Oceanic Technol.* 7, 19–37.
- Longuet-Higgins, M.S., Stewart, R.W., 1962. Radiation stress and mass transport in surface gravity waves with application to surf beats. *J. Fluid Mech.* 13 (4), 481–504.
- MacMahan, J.H., Reniers, A.J.H.M., Thornton, E.B., 2010. Vortical surf zone velocity fluctuations with O(10) min period. *J. Geophys. Res.* 115, C06007. p. 18.
- Magnell, B.A., Signorini, S.R., 1986. Fall 1984 Delaware Bay Acoustic Doppler Profiler Intercomparison Experiment. In: Appell, G.F., Woodward, W.E. (Eds.), Proc. IEEE Third Working Conference on Current Measurement. IEEE, New York, NY, USA, pp. 122–152. January 22–24, 1986, Airlie, VA.
- Mahapatra, P.R., Zrnic, D.S., 1983. Practical algorithms for mean velocity estimation in pulse Doppler weather radars using a small number of samples. *IEEE Trans. Geosci. Remote Sensing GE-21*, 491–501.
- Munchow, A., Coughran, C.S., Hendershott, M.C., Winant, C.D., 1995. Performance and calibration of an acoustic Doppler current profiler towed below the surface. *J. Atmos. Oceanic Technol.* 12, 435–444.
- New, A.L., 1992. Factors affecting the quality of shipboard acoustic Doppler current profiler data. *Deep-Sea Res.* 39, 1985–1992.
- Okuno, K., Tsuji, Y., Hisamoto, S., Okino, M., Emura, T., 1983. Three-dimensional current and scattering strength distribution mapping system. Proc. IEEE Oceans '83. New York, NY, USA, 301–305.
- Pawka, S.S., 1983. Island shadows in wave directional spectra. *J. Geophys. Res.* 88, 2579–2591.
- Pedersen, T., Lohrmann, A., 2004. Possibilities and limitations of acoustic surface tracking. Proc. Oceans 2004. Kobe, Japan.
- Perkins, H., de Strobel, F., Gualdesi, L., 2000. The barny sentinel trawl-resistant ADCP bottom mount: Design, testing, and application. *IEEE J. Oceanic Eng.* 25 (4), 430–436.
- Pettigrew, N.R., Irish, J.D., 1983. An evaluation of a bottom mounted Doppler acoustic profiling current meter. Proc. IEEE Oceans '83, 182–186.
- Pettigrew, N.R., Beardsley, R.C., Irish, J.D., 1986. Field evaluations of a bottom mounted acoustic Doppler profiler and conventional current meter moorings. In: Appell, G.F., Woodward, W.E. (Eds.), Proc. IEEE Third Working Conference on Current Measurement. IEEE, New York, NY, USA, pp. 153–162. January 22–24, 1986, Airlie, VA.
- Peynaud, F., Pijanowski, J., 1979. An acoustic Doppler current meter, OTC 3457. Proc. Offshore Technology Conference, 863–867.
- Pinkel, R., 1980. Acoustic Doppler techniques. In: Dobson, F., Hasse, L., Davis, R. (Eds.), Air-sea interaction: Instruments and methods. Plenum Press, New York, NY, USA, pp. 171–199.
- Pinkel, R., Smith, J., 1992. Repeat sequence codes for improved performance of Doppler sounders. *J. Atmos. Oceanic Technol.* 9, 149–163.
- Pollard, R.T., Reed, J.F., 1989. A method of calibrating ship-mounted acoustic Doppler current profilers and the limitations of gyro compasses. *J. Atmos. Oceanic Technol.* 6, 859–865.
- Pulkkinen, K., 1993. Comparison of different bin-mapping methods for a bottom-mounted acoustic profiler. *J. Atmos. Oceanic Technol.* 10, 404–409.
- Pullen, P.E., McPhaden, M.J., Freitag, H.P., Gast, J., 1992. Surface wave induced skew errors in Acoustic Doppler Current Profiler measurements from high shear regimes. In: Proc. IEEE Conference, Oceans '92. IEEE, New York, NY, USA, pp. 706–711.
- Reniers, A.J.H.M., et al., 2009. Surf zone surface retention on a rip-channelled beach. *J. Geophys. Res.* 114.
- Reniers, A.J.H.M., Roelvink, J.A., Thornton, E.B., 2004. Morphodynamic modeling of an embayed beach under wave group forcing. *J. Geophys. Res.* 109.
- Rowe, F.D., Young, J.W., 1979. An ocean current profiler using Doppler sonar, IEEE Proceedings. Oceans '79, 292–297.
- Rowe, F.D., Deines, K.L., Gordon, R.L., 1986. High resolution current profiler. In: Appell, G.F., Woodward, W.E. (Eds.), Proc. IEEE Third Working Conference on Current Measurement. IEEE, New York, NY, USA, pp. 184–189. January 22–24, 1986, Airlie, VA.
- Sato, S., Nakamura, T., Kawanabe, M., 1999. Horizontal ADCP, new instrument for measuring current speed in a horizontal plane. *Proc. IEEE*, 121–124.
- Schott, 1986. Medium-range vertical acoustic Doppler current profiling from submerged buoys. *Deep-Sea Res.* 33, 1279–1292.
- Schott, F., 1986. Medium-range Vertical acoustic Doppler current profiling from submerged buoys. Rosenstiel school of Marine and Atmospheric Science, University of Miami, Miami, FL, USA. presented orally at the IEEE Third Working conference on current measurement.
- Schott, F., 1986. Medium-range vertical acoustic Doppler current profiling from submerged buoys. *Deep-Sea Res.* 33A, 1279–1292.
- Schott, F., Johns, W., 1987. Half-year long measurements with a buoy mounted acoustic Doppler current profiler in the Somali Current. *J. Geophys. Res.* 92, 5169–5176.
- Siegel, E., 2007. New methods for subsurface wave measurements at offshore locations. *Ocean News & Technology* 13 (6), 38–39.
- Sirmans, D., Bumgarner, B., 1975. Numerical comparison of five mean frequency estimators. *J. Applied Meteor.* 14, 991–1003.
- Skelin, D., Public, I., Vukadin, P., 2008. Current profile measurement using moored acoustic Doppler current profiler. Proc. 50th International Symposium ELMAR-2008, September 10–12, 2008, Zadar, Croatia, 411–414.
- Soulsby, R.L., 1980. Selecting record length and digitization rate for near-bed turbulence measurements. *J. Physical Oceanography* 10 (2), 208–219.
- Spain, P.F., Dorson, D.L., Rossby, H.T., 1981. Pegasus: A simple, acoustically tracked velocity profiler. *Deep-Sea Res.* 28A, 1553–1567.
- Strong, B., Devine, P., 2000. Now use ADCPs for waves as well as currents. *International Ocean Systems* 4 (5), 4–8.
- Strong, B., Brumley, B., Stone, G.W., Zhang, X., 2003. The application of the Doppler shifted dispersion relationship to hurricane wave data from an ADCP directional wave gauge and co-located pressure

- sensor. Proc. of the IEEE/OES Seventh Working Conference on Current Measurement Technology, 119–124.
- Terray, E.A., Brumley, B.H., Strong, B., 1999. Measuring waves and currents with an upward-looking ADCP. In: Proc. IEEE Sixth Working Conference on Current Measurement. IEEE, pp. 66–71.
- Terray, E.A., Krogstad, H.E., Cabrera, R., Gordon, R.L., Lohrmann, A., 1990. Measuring wave direction using upward-looking Doppler sonar. In: Appell, G.F., Curtin, T.B. (Eds.), Proc. of the IEEE 4th Working Conf. on Current Measurement. IEEE Press, New York. (IEEE Catalog No. 90CH2861–3), 252–257.
- Terray, E.A., Gordon, R.L., Brumley, B.H., 1997. Measuring wave height and direction using upward-looking ADCPs. Proc. of Oceans '97. MTS/IEEE, 287–290.
- Theriault, K.B., 1986a. Incoherent multibeam Doppler current profiler performance: Part I—Estimated variance. IEEE J. Oceanic Eng. OE-11, 7–15.
- Theriault, K.B., 1986b. Incoherent multibeam Doppler current profiler performance: Part II, Spatial response. IEEE J. Oceanic Eng. OE-11, 16–25.
- Thomson, R.E., Gordon, R.L., Dymond, J., 1989. Acoustic Doppler current profiler observations of a mid-ocean ridge hydrothermal plume. J. Geophys. Res. 94, 4709–4720.
- Thorpe, S.A., 1986. Measurements with an automatically recording inverted echo sounder; ARIES and the bubble clouds. J. Phys. Oceanogr. 16, 1462–1478.
- Trevorrow, M.V., Farmer, D.M., 1992. The use of Barker codes in Doppler sonar measurements. J. Atmos. Oceanic Technol. 9, 699–704.
- Trump, C.L., 1986. Estimating absolute current velocities by merging shipboard Doppler current profiler data with Loran C data. In: Appell, G.F., Woodward, W.E. (Eds.), Proc. IEEE Third Working Conference on Current Measurement. IEEE, New York, NY, USA, pp. 177–183. January 22–24, 1986, Airlie, VA.
- Trump, C.L., Okawa, B.S., Hill, R.H., 1985. The characterization of a midocean front with a Doppler shear profiler and a thermistor chain. J. Atmos. Oceanic Technol. 2, 508–516.
- Urick, R.J., 1982. Principles of Underwater Sound, third ed. McGraw-Hill, New York, NY, USA.
- Urick, R.J., 1996. Principles of underwater sound, third ed. Peninsula Publishing, Los Altos, CA, USA.
- Visbeck, M., Fischer, J., 1995. Sea surface conditions remotely sensed by upward-looking ADCPs. J. Atmos. Oceanic Technol. 12, 141–149.
- Wilson, W.D., 1994. Deep ocean current profiling with a lowered broadband acoustic Doppler current profiler. In: 1994 IEEE. I-660–I-665.
- Zedel, L., 1994. Deep ocean wave measurements using a vertically oriented sonar. J. Atmos. Oceanic Technol. 11 (1), 182–191.
- Zedel, L.J., Church, J.A., 1987. Real time screening techniques for Doppler current profiler data. J. Atmos. Oceanic. Technol. 4, 572–581.
- Zhang, Y., Willcox, J.S., 1997. Current velocity mapping using an AUV-borne acoustic Doppler current profiler. In: Proc. 10th International Symposium on Unmanned Untethered Submersible Technology. Durban, NH, USA, Sept. 1997, pp. 31–40.
- Anderson, S.P., Matthews, P., 2005. A towed 75 kHz ADCP for operational deepwater current surveys. Proc. IEEE/OES Eighth Working Conference on Current Measurement Technology, 46–49.
- Appell, G.F., 1984. A real-time current measurement system. Sea Technol. 25.
- Appell, G.F., Mero, T.N., Sprenke, J.J., Schmidt, D.R., 1985. An inter-comparison of two acoustic Doppler current profilers. Oceans '85 Conference Record. IEEE, New York, NY, USA, 723–730.
- Beck, S., Pinkel, R., Morison, J., 1986. Doppler acoustic velocity profiling in the Arctic. In: Proceedings of the IEEE Third Working Conference on Current Measurement. January 22–24, 1986, Airlie, VA, IEEE, New York, NY, USA.
- Chern, C., Wang, J., 2003. Numerical study of the upper-layer circulation in the South China Sea. J. Oceanogr. 59, 11–24.
- Derecki, J.A., Quinn, F.H., 1985. Use of current meters for continuous measurement of flows in large rivers. EOS 66, 907.
- Didden, N., 1989. Performance evaluation of a shipboard 115-kHz acoustic Doppler current profiler. Cont. Shelf Res. 7, 1232–1243.
- Fischer, J., Visbeck, M., 1993. Deep velocity profiling with self-contained ADCPs. J. Atmos. Oceanic Technol. 10, 764–773.
- Gordon, R.L., Skorstad, H.E., 1985. North Sea data will upgrade platform designs. Ocean Industry. July 1985, 35–39.
- Irish, J.D., Pettigrew, N.R., Deines, K., Rowe, F., 1983. A new bottom-mounted, internally recording Doppler acoustic profiling current meter. IEEE Proceedings of the Third Working Symposium on Oceanographic Data Systems. IEEE, New York, NY, USA, 109–113.
- Johns, W.E., 1988. Near-surface current measurements in the Gulf Stream using an upward looking Acoustic Doppler Current Profiler. J. Atmos. Oceanic. Technol. 5, 602–613.
- Kosro, P.M., 1985. Accuracy of shipboard Doppler current profiling during CODE. In: Proceedings of the IEEE Third Working Conference on Current Measurement. January 22–24, 1986, Airlie, VA, IEEE, New York, NY, USA.
- Kosro, P.M., 1985. Shipboard acoustic current profiling during the Coastal Ocean Dynamics Experiment. Ph.D. thesis. Scripps Institution of Oceanography, SIO, Reference No. 85–8, La Jolla, CA, United States.
- Kosro, P.M., 1985. Shipboard acoustic Doppler current profiling during CODE. SIO Ref. 85–5, La Jolla, CA, United States.
- Krogstad, H.E., Gordon, R.L., Miller, M.C., 1988. High resolution directional wave spectra from horizontally mounted acoustic Doppler current meters. J. Atmos. Ocean. Technol. 5, 340–352.
- Leaman, K.D., Sanford, T.B., 1975. Vertical energy propagation of inertial waves: a vector spectral analysis of velocity profiles. J. Geophys. Res. 80, 1975–1978.
- Luyten, J.R., Swallow, J.C., 1976. Equatorial undercurrents. Deep-Sea Res. 23, 999–1001.
- Magnell, B., Signorini, S., 1986. Proceedings of the IEEE Third Working Conference on Current Measurement. Performance of an RDI acoustic Doppler profiler in an intercomparison experiment in Delaware Bay. January 22–24, 1986, Airlie, VA, IEEE, New York, NY, USA.
- National Ocean Service, 2001. Tidal Current Tables 2002, Atlantic Coast of North America. U.S. Department of Commerce, National Oceanic and Atmospheric Administration.
- Pettigrew, N.R., Irish, J.D., 1983. An evaluation of a bottom-mounted Doppler acoustic profiling current meter, Proceedings of Oceans '83. IEEE, New York, NY, USA.

BIBLIOGRAPHY

- Alderson, S.G., Cunningham, S.A., 1999. Velocity errors in Acoustic Doppler Current Profiler measurements due to platform attitude variations and their effect on volume transport estimates. J. Atmos. Ocean. Technol. 16, 96–106.

- Pettigrew, N.R., Irish, J.D., Beardsley, R.C., 1983. An intercomparison of a bottom-mounted Doppler acoustic profiling current meter and a conventional current meter mooring. *EOS* 69, 251.
- Pettigrew, N.R., Beardsley, R.C., Irish, J.D., 1986. Field evaluations of a bottom-mounted acoustic Doppler profiler and a conventional current meter moorings. In: Proceedings of the IEEE Third Working Conference on Current Measurement. IEEE, New York, NY, USA. January 22–24, 1986, Airlie, VA.
- Pinkel, R., Smith, J.A., 1987. Open ocean surface wave measurement using Doppler sonar. *J. Geophys. Res.* 92, 12,967–12,973.
- Porter, D.L., Williams, R.G., Swassing, C.M., 1986. An intercomparison of surface circulation in the Delaware Bay obtained from CODAR, drifting transponders, and RADS. In: Proceedings of the IEEE Third Working Conference on Current Measurement. IEEE, New York, NY, USA. January 22–24, 1986, Airlie, VA.
- Rowe, F.D., Deines, K.L., Gordon, R.L., 1986. High resolution current profiler. In: Proceedings of the IEEE Third Working Conference on Current Measurement. IEEE, New York, NY, USA. January 22–24, 1986, Airlie, VA.
- Simpson, M.R., 1986. Evaluation of a vessel-mounted acoustic Doppler current profiler for use in rivers and estuaries. In: Proceedings of the IEEE Third Working Conference on Current Measurement. IEEE, New York, NY, USA. January 22–24, 1986, Airlie, VA.
- Smith, J.A., 1989. Doppler sonar and surface waves: Range and resolution. *J. Atmos. Ocean. Technol.* 6, 680–696.
- Stanway, M.J., 2010. Water profile navigation with an Acoustic Doppler Current Profiler. In: 2010 IEEE.
- Strong, B., Brumley, B., Terray, E.A., Kraus, N.C., 2000. Validation of the Doppler shifted dispersion relation for waves in the presence of strong tidal currents, using ADCP wave directional spectra and comparison data. Proc. 6th Intl. Workshop on Wave Hindcasting and Forecasting, November 6–10, 2000, Monterey, CA, USA.
- Strong, B., Brumley, B., Terray, E.A., Stone, G.W., 2000. The performance of ADCP-derived wave spectra and comparison with other independent measurements. Cesena (FC), Italy. www.rdinstruments.com/library.html.
- Terray, E.A., Brumley, B.H., Strong, B., 1999. Measuring waves and currents with an upward-looking ADCP. Proc. IEEE 6th Working Conference on Current Measurement, 66–71. IEEE Press.
- Terray, E.A., Gordon, R.L., Brumley, B.H., 1997. Measuring wave height and direction using upward-looking ADCPs, Proc. Oceans '97, MTS / IEEE, 287–290.
- Trump, C.L., 1986. Estimating absolute current velocities by merging ship-board Doppler current profiler data with Loran-C data. In: Proceedings of the IEEE Third Working Conference on Current Measurement. January 22–24, 1986, Airlie, VA, IEEE, New York, NY, USA.
- Wilson, P., 2009. Measurement of the marine energy resource: Practical solutions for an expectant industry. Part 1: Tidal energy. *International Ocean Systems* 13 (2), 22–25.
- Wolff, P.M., Konop, D., 1984. Predicting water circulation in Delaware Bay and River: NOAA's new approach. *Sea Technology*. Sept. 1984, 18–22.
- Work, P.A., 2008. Nearshore directional wave measurements by surface-following buoy and acoustic Doppler current profiler. *Ocean Engineering* 35, 727–737.